ENVISAT GOMOS Monthly report: November 2004

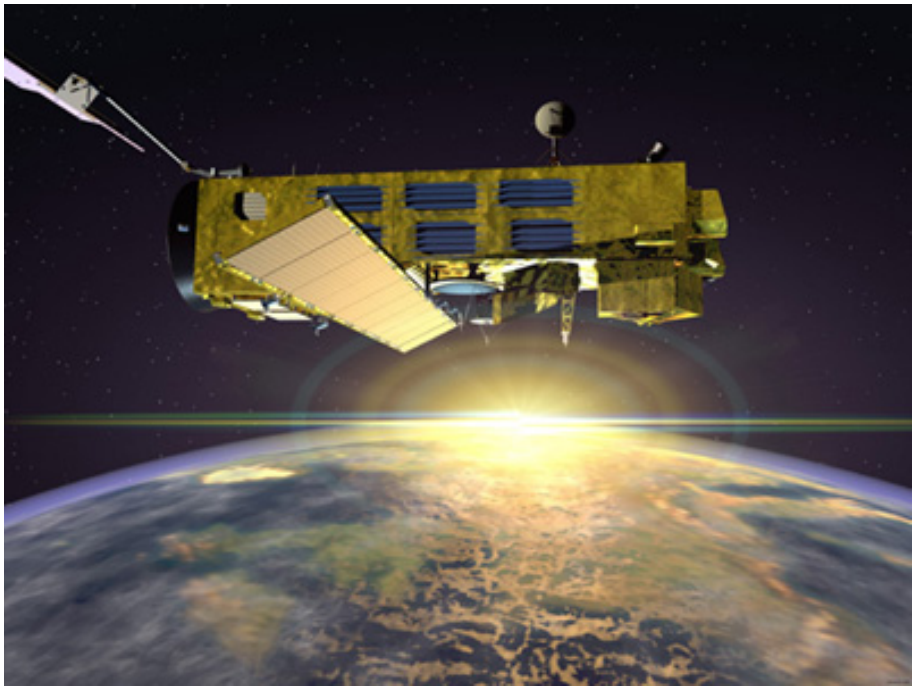

Prepared by:	PCF Team	ESA EOP-GOQ
Inputs from:	GOMOS Quality Working Group, ECMWF	
Issue:	1.0	
Reference:	ENVI-SPPA-EOPG-TN-04-00033	
Date of issue:	17 December 2004	
Status:	Reviewed	
Document type:	Technical Note	
Approved by:	Rob Koopman	

TABLE OF CONTENTS

1 INTRODUCTION

The GOMOS monthly report documents the current status and recent changes to the GOMOS instrument, its data processing chain, and its data products.
The Monthly Report (hereafter MR) is composed of analysis results obtained by the Product Control Facility, combined with inputs received from the different entities working on GOMOS operation, calibration, product validation and data quality. These teams participate in the GOMOS Quality Working Group:

- European Space Agency (ESRIN-PCF, ESOC, ESTEC-PLSO)
- ACRI
- Service d'Aeronomie
- Finnish Meteorological Institute
- IASB-Belgian Institute for Space Aeronomy
- Astrium Space
- ECMWF

In addition, the group interfaces with the Atmospheric Chemistry Validation Team.

1.1 Scope

The main objective of the Monthly Report is to give, on a regular basis, the status of GOMOS instrument performance, data acquisition, results of anomaly investigations, calibration activities and validation campaigns. The following six sections compose the MR:

- Summary
- Unavailability
- Instrument Performance and Configuration
- Level 1 Product Quality Monitoring
- Level 2 Product Quality Monitoring
- Validation Activities and Results

1.2 References

[1] ENVISAT Weekly Mission Operations Report #125, #126, #127, #128, #129 ENVI-ESOC-OPS-RP-1011-TOS-OF
[2] 'Level 1b Detailed Processing Model', PO-RS-ACR-GS-0001, issue 6.1, 28 Nov, 2003
[3] 'Level 2 Detailed Processing Model', PO-RS-ACR-GS-0002, issue 6.0, 6 Feb, 2004
[4] ECMWF GOMOS Monthly Reports

1.3 Acronyms and Abbreviations

ACVT Atmospheric Chemistry Validation Team

ADF	Auxiliary Data File
ADS	Auxiliary Data Server
ANX	Ascending Node Crossing
ARF	Archiving Facility (PDS)
CCU	Central Communication Unit
CFS	CCU Flight Software
CNES	Centre National d'Études Spatiales
CTI	Configuration Table Interface / Configurable Transfer Item
CR	Cyclic Report
DC	Dark Charge
DMOP	Detailed Mission Operation Plan
DPM	Detailed Processing Model
DS	Data Server
DSA	Dark Sky Area
DSD	Data Set Descriptor
ECMWF	European Centre for Medium Weather Forecast
EQSOL	Equipment Switch Off Line
ESA	European Space Agency
ESL	Expert Support Laboratory
ESRIN	European Space Research Institute
ESTEC	European Space Research & Technology Centre
ESOC	European Space Operations Centre
FCM	Fine Control Mode
FMI	Finnish Meteorological Institute
FOCC	Flight Operations Control Centre (ENVISAT)
FP1	Fast Photometer 1
FP2	Fast Photometer 2
GADS	Global Annotations Data Set
GOMOS	Global Ozone Monitoring by Occultation of Stars
GOPR	GOmos PRototype
GS	Ground Segment
HK	Housekeeping
IASB	Institut d'Aeronomie Spatiale de Belgique
IAT	Interactive Analysis Tool
ICU	Instrument Control Unit
IDL	Interactive Data Language
IECF	Instrument Engineering and Calibration Facilities
IMK	Institute of Meteorology Karlsruhe (Meteorologisch Institut Karlsuhe)
INV	Inventory Facilities (PDS)
IPF	Instrument Processing Facilities (PDS)
JPL	Jet Propulsion Laboratory
LAN	Local Area Network
LMA	Levenberg-Marquardt Algorithm
LPCE	Laboratoire de Physique et Chimie de l'Environnement
LUT	Look Up Table
MCMD	Macro Command
MDE	Mechanism Drive Electronics
MIP	Most Illuminated Pixel

MPH	Main Product Header
MPS	Mission Planning System
MR	Monthly Report
OBT	On Board Time
OCM	Orbit Control Manoeuvre
OOP	Out-of-plane
OP	Operational Phase of ENVISAT
PAC	Processing and Archiving Centre (PDS)
PCF	Product Control Facility
PDCC	Payload Data Control Centre (PDS)
PDHS	Payload Data Handling Station (PDS)
PDHS-E	Payload Data Handling Station – ESRIN
PDHS-K	Payload Data Handling Station – Kiruna
PDS	Payload Data Segment
PEB	Payload Equipment Bay
PLSOL	Payload Switch off Line
PMC	Payload Module Computer
PRNU	Pixel Response Non Uniformity
PSO	On-Orbit Position
QC	Quality Control
QUARC	Quality Analysis and Reporting Computer
QWG	Quality Working Group
RIVM	Rijksinstituut voor Volksgezondheid en Milieu
RTS	Random Telegraphic Signal
SA	Service d'Aeronomie
SAA	South Atlantic Anomaly
SATU	Star Acquisition and Tracking Unit
SFA	Steering Front Assembly
SFCM	Stellar Fine Control Mode
SFM	Steering Front Mechanism
SMNA	Servicio Meteorológico Nacional de Argentina
SODAP	Switch On and Data Acquisition Phase
SPA1	Spectrometer A CCD 1
SPA2	Spectrometer A CCD 2
SPB1	Spectrometer B CCD 1
SPB2	Spectrometer B CCD 2
SPH	Specific Product Header
SQADS	Summary Quality Annotation Data Set
SSP	Sun Shade Position
SZA	Solar Zenith Angle

2 SUMMARY

During the reporting period GOMOS instrument had one planned unavailability period on 11th Nov 2004 23:40:00 until 12th Nov 2004 02:21:00 due to a Fine Orbit Control Manoeuvre. For the rest of the period, GOMOS has been operating nominally (section 3.1).

Starting from orbit 14139 (on the 12th November at around 20:08) to orbit 14196 (on the 16th of November at around 19:43) all ESRIN orbits had GOMOS data with lots of missing packets. This anomaly affected all PDHS-E generated products and was caused by antenna transmission failures on the operational "I" channel, while the "Q" channel was completely nominal. Unfortunately there were also random failures on the backup chain preventing the recovery of some orbits that have to be considered lost (section 4).

On 9th November 09:43 -18:07 the instrument was measuring at tangent altitudes between 310-100 km (nominal range is 130-5 km) due to a special Quality Working Group request coming from ACRI institute for the study of the reflectivity. This means that the data between those dates are not suitable for any user application (section 4.1).

The level 0 availability is high during the reporting period, and presented a decrease on the 2nd week of November: orbits 14097 until mid 14102 are missing. For level 1b data, availability is decreased from 95% to 88% since the 2nd week until the end of the month (section 3.3).

The detector temperatures during November are one degree greater than the ones registered during the same period in 2003 (global increase due to the radiator ageing). The expected seasonal variation of the temperatures with amplitude of around one degree can be clearly observed. The peaks that occur mainly in spectrometer B1 and B2 are also to be noted. They happen for some consecutive occultations and every 8-10 days (section 4.3).

From orbit 14132 until orbit 14200 a gradual increase in elevation MIP corresponding to a total mispointing of 20 mdeg is observed. This local increase has no impact on the operations of GOMOS (section 4.6.3).

The radiometric sensitivity monitoring shows values outside the warning threshold set to 10% for the photometers, and investigations were performed by the QWG. For stars 9 and 18 only very few points are the cause of the big variation of the percentage meaning that there is not a real problem in the radiometric sensitivity of the photometers. For star id 25, the problem is different. It is observed a real variation of the ratios but as it is only seen for this star, it can be concluded that the variation should be linked to the star itself and not to the photometers. For star 25 also the UV ratio is greater than 10%. It is clear that there is a global decrease of UV ratios for all the stars confirming the expected degradation suffered by the UV optics. Anyway, this variation is very small considering also the small variation for the rest of the stars used for this monitoring (section 5.4-1).

Section 4.2 is a new chapter included in the monthly report with the objective of clarifying a confusing issue like the limb and the illumination conditions in GOMOS data. To have these ideas clear is very important to the user because the illumination condition is directly related to the quality of the data to be used by any user application.

On 2nd, 8th, 15th, 22nd and 29th November new calibration ADF's were disseminated with updated DC maps of orbits 13864, 13977, 14064, 14164, 14264 and 14365 respectively (section 5.1.2)

3 INSTRUMENT UNAVAILABILITY

3.1 GOMOS Unavailability Periods

In table 3.1-1 there is the only GOMOS unavailability report issued during the period 1st November (00:00:00) until 30th November 2004.

Table 3.1-1: List of unavailability periods issued during the reporting month

Reference of unavailability report	Start time Star orbit	Stop time Stop orbit	Description
EN-UNA-2004/0273	11 Nov 2004 23:40:00.000 Orbit = 14126	12 Nov 2004 02:21:00.000 Orbit = 14128	Planned FCM

3.2 Stars Lost in Centering

The acquisition of a star initiates with a rallying phase where the telescope mechanism is directed towards the expected position of the star. Subsequently the acquisition procedure enters into detection mode, where the SATU star tracker output signal is pre-processed for spot presence survey and for the location of the most illuminated couple of adjacent pixels for two added lines, over the detection field. The Most Illuminated Pixel (MIP) defines the position of the first SATU centering window. The next step in the acquisition sequence is then initiated and consists of a centering phase where the SATU output signal is pre-processed for spot presence survey over the maximum of 10x10 pixel field. This allows the third phase to begin: the tracking phase.

The centering phase has occasionally resulted in loss of the star from the field of view. The fig. 3.2-1 reports the percentage of the stars lost in centering for the period 03-FEB-2003 to 28-NOV-2004. It can be seen that three stars, mainly weak stars (higher star id means higher magnitude) are lost during centering phase between 4 and 6 % of their planned observations. The star id 115 was lost 40% of the times but it was planned to be occulted five times and was lost twice (in period 26th January – 1st February), so this high percentage of loss is not statistically significant.

As the monitoring shows neither trend nor excessively high percentages of loss, there is no need for the moment to reject any star from the catalogue, and there is no indication of instrument-related problems. However, this month there were 10 instances of “target not detected” (3 times x 152, 175, 107, 180 x 3, 99, and 100) whereas the usual statistics is just one or two instances per month. This phenomenon will be carefully monitored in order to check if this new trend continues during the following months.

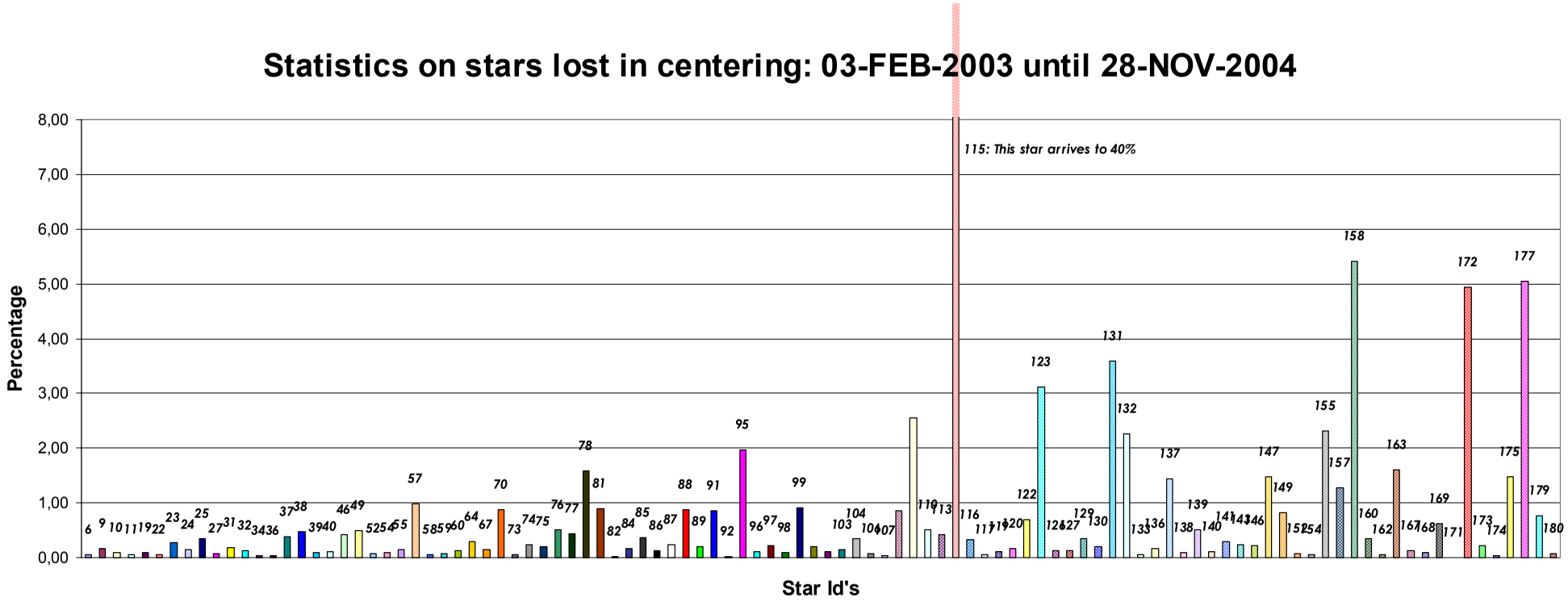

Figure 3.2-1: Statistics on stars that have been lost during the centering phase. The number above the columns correspond to the Star ID

3.3 Data Generation Gaps

The trend in percentage of available data within the archives PDHS-K and PDHS-E is depicted in fig. 3.3-1 (when instrument was in operation). It is a good indicator on how the PDS chain is working in terms of generation and dissemination of data to the archives. The percentage is calculated once per week.

The level 0 availability is high during the reporting period and presented a decrease on the 2nd week of November: orbits 14097 until mid 14102 are missing. For level 1b data, availability is decreased from 95% to 88% since the 2nd week until the end of the month.

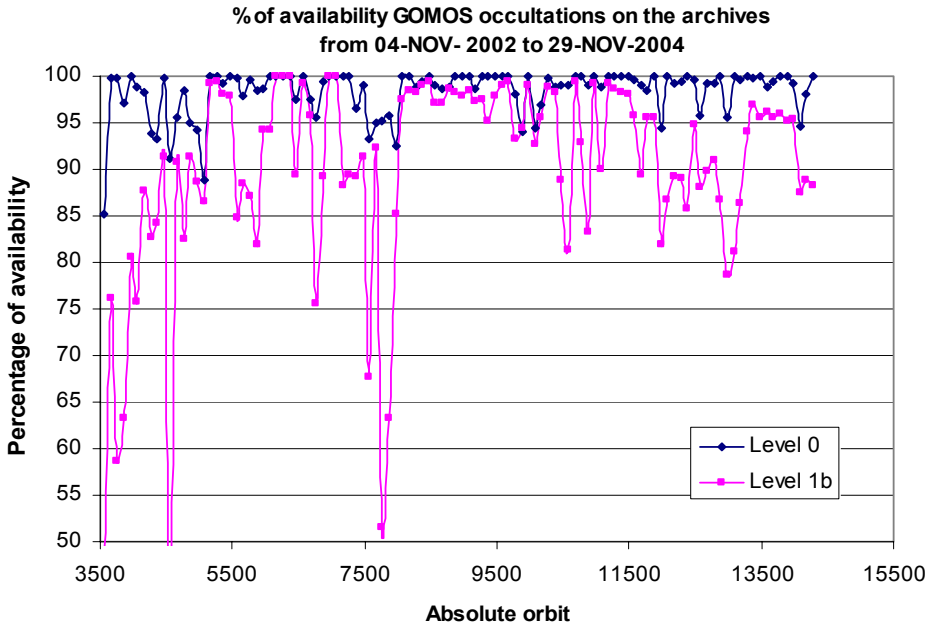

Figure 3.3-1: Percentage of level 0 and level 1b data availability on the archives PDHS-E and PDHS-K

3.3.1 LEVEL 0 PRODUCTS: GOM_NL__0P

Occultations planned to be acquired but for which no GOM_NL__0P data product has become available are presented in fig. 3.3-2 for the reporting period.

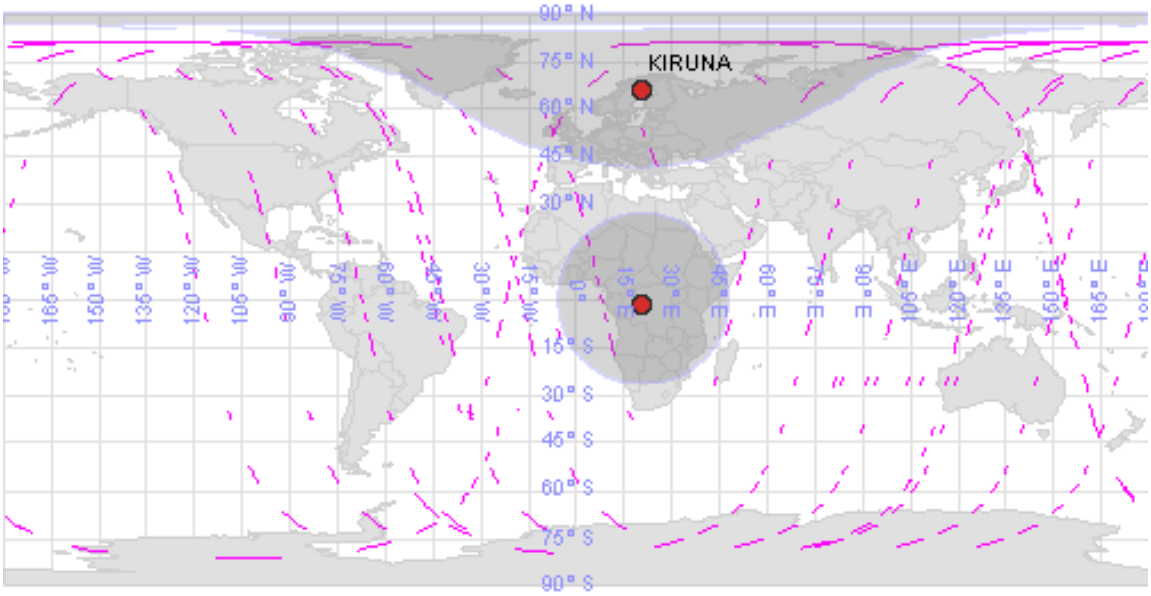

Figure 3.3-2: The pink lines are the orbit segments corresponding to planned data acquisitions for which no GOMOS level 0 product has become available. The grey shadow centered in Kiruna represents the visibility of the station. The grey shadow centered in Africa represents the ARTEMIS satellite nominal position

3.3.2 HIGHER LEVEL PRODUCTS

Routine dissemination of higher-level products produced by the PDS to Cal/Val teams and other users is enabled. Currently ESA is also providing products that are reprocessed with the prototype processor developed and operated by ACRI.

4 INSTRUMENT CONFIGURATION AND PERFORMANCE

Starting from orbit 14139 (on the 12th November at around 20:08) to orbit 14196 (on the 16th of November at around 19:43) all ESRIN orbits had GOMOS data with lots of missing packets. This anomaly affected all PDHS-E generated products and was caused by "I" channel acquisition failures on the operational chain, while the "Q" channel was completely nominal. Unfortunately there were also random failures on the backup chain preventing the recovery of some orbits that have to be considered lost (see table 3.3-1).

Table 3.3-1: Recovery strategy after "I" channel acquisition failure on 12th November 2004

ORBIT	AOS	SYSTEM	PROCESSING
14188	16/11/2004 06:37	LR1	RECOVERABLE
14187	16/11/2004 04:55	LR1	RECOVERABLE
14186	16/11/2004 03:21	LR1	RECOVERABLE
14185	16/11/2004 01:52	LR1	RECOVERABLE
14185	16/11/2004 02:02	LR1	NOT RECOVERABLE
14184	16/11/2004 00:33	LR1	RECOVERABLE
14183	16/11/2004 23:04	LR1	RECOVERABLE
14182	16/11/2004 21:12	LR1	RECOVERABLE
14181	15/11/2004 19:38	LR1	RECOVERABLE
14180	15/11/2004 17:52	LR1	RECOVERABLE
14179	15/11/2004 16:19	LR1	RECOVERABLE
14177	15/11/2004 12:26	LR1	NOT RECOVERABLE
14176	15/11/2004 10:38	LR1	RECOVERABLE
14173	15/11/2004 05:27	LR1	RECOVERABLE
14172	15/11/2004 03:48	LR1	RECOVERABLE
14171	15/11/2004 02:28	LR1	RECOVERABLE
14170	15/11/2004 00:55	LR1	RECOVERABLE
14169	14/11/2004 23:36	LR1	RECOVERABLE
14168	14/11/2004 21:55	LR1	NOT RECOVERABLE
14167	14/11/2004 20:08	LR1	NOT RECOVERABLE
14166	14/11/2004 18:32	LR1	RECOVERABLE
14165	14/11/2004 16:43	LR1	RECOVERABLE
14163	14/11/2004 12:42	LR1	RECOVERABLE
14162	14/11/2004 10:47	LR1	RECOVERABLE
14162	14/11/2004 11:09	LR1	RECOVERABLE
14159	14/11/2004 06:00	LR1	RECOVERABLE
14158	14/11/2004 04:17	LR1	RECOVERABLE
14157	14/11/2004 02:43	LR1	RECOVERABLE
14156	14/11/2004 01:41	LR1	RECOVERABLE
14155	14/11/2004 00:07	LR1	RECOVERABLE
14154	13/11/2004 22:27	LR1	RECOVERABLE
14153	13/11/2004 20:43	LR1	RECOVERABLE
14152	13/11/2004 18:55	LR1	NOT RECOVERABLE
14151	13/11/2004 17:26	LR1	RECOVERABLE
14150	13/11/2004 15:33	LR1	RECOVERABLE
14148	13/11/2004 11:34	LR1	RECOVERABLE
14145	13/11/2004 06:35	LR1	RECOVERABLE
14144	13/11/2004 04:51	LR1	RECOVERABLE
14143	13/11/2004 03:15	LR1	NOT RECOVERABLE
14142	13/11/2004 01:47	LR1	NOT RECOVERABLE
14142	13/11/2004 02:15	LR1	NOT RECOVERABLE
14141	13/11/2004 00:35	LR1	NOT RECOVERABLE
14140	12/11/2004 22:28	LR1	RECOVERABLE
14138	12/11/2004 19:38	LR1	NOT RECOVERABLE
14137	12/11/2004 17:58	LR1	RECOVERABLE
14136	12/11/2004 16:02	LR1	RECOVERABLE
14134	12/11/2004 12:07	LR1	RECOVERABLE
14133	12/11/2004 10:32	LR1	NOT RECOVERABLE
14133	12/11/2004 10:59	LR1	RECOVERABLE
14130	12/11/2004 05:21	LR1	RECOVERABLE
14129	12/11/2004 03:42	LR1	NOT RECOVERABLE

4.1 Instrument Operation and Configuration

During the period end of March 2003 to July 2003 the azimuth range had to be decreased in steps (table 4.1-1) to avoid an instrument problem ("Voice_coil_command_saturation" anomaly) that caused GOMOS to go into STAND BY/REFUSE mode. On July 2003 the driver assembly was switched to the redundant B-side and since that date the full azimuth range (-10.8, +90.8) is again available.

Table 4.1-1: Historical changes in Azimuth configuration

Date	Orbit	Minimum Azimuth	Maximum Azimuth
29-MAR-2003 17:40	5635	0.0	+90.8
31-MAY-2003 06:22	6530	+4.0	+90.8
16-JUN-2003 16:17	6765	+12.0	+90.8
15-JUL-2003 01:39	7200	-10.8	+90.8

The operations of the instrument in other modes than occultation mode are identified in table 4.1-2. On 9th November 09:43 -18:07 the instrument was measuring at tangent altitudes between 310-100 km (nominal range is 130-5 km) due to a special request coming from ACRI institute for the study of the reflectivity. This means that the data between those dates are not suitable for any user application.

There was no new Configurable Table Interface (CTI) uploaded to the instrument. The files used since the beginning of the mission are in table 4.1-3.

Table 4.1-2: GOMOS operations during the reporting period

UTC time	Start orbit	Stop orbit	Mode (Asynchronous or Synchronous)	Calibration (CAL) or Dark Sky Area (DSA)
06 NOV 2004 01.14.56	14042	14049	A	CAL67
09 NOV 2004 09.43.41	14090	14094	S	Measurements between 310-100 km (special request from ACRI). Nominal range is 130-5 km.

Table 4.1-3: Historic CTI Tables

CTI filename	Dissemination to FOCC
CTI_SMP_GMVIEC20030716_123904_00000000_00000004_20030715_000000_20781231_235959.N1	16-JUL-2003
CTI_SMP_GMVIEC20021104_075734_00000000_00000003_20021002_000000_20781231_235959.N1	06-NOV-2003
CTI_SMP_GMVIEC20021002_082339_00000000_00000002_20021002_000000_20781231_235959.N1	07-OCT-2003
CTI_SMP_GMVIEC20020207_154455_00000000_00000000_20020301_032709_20781231_235959.N1	21-FEB-2002

4.2 Limb, Illumination conditions and instrument gain setting

The **limb** and the **illumination condition** are two parameters that can confuse the user community. In table 4.2-1 there are specified the product (level 1b and level 2) parameter where the flag is located, the meaning and the source. The difference between the limb (SPH/bright_limb) and the illumination condition (SUMMARY_QUALITY/limb_flag) is that the first one is coming from the mission scenario and the second is coming from the processing (sun zenith angle computed). The SPH/bright_limb is for some occultations set to "dark" in the mission scenario while they are in fact in bright limb illumination conditions. To select highest quality data for scientific application, data with SUMMARY_QUALITY/limb_flag equal to '0' should be used (see also the disclaimer:

http://envisat.esa.int/dataproducts/availability/disclaimers). The instrument gain settings are also specified in table 4.2-1 (they depend on the mission scenario flags) just for information completeness.

Table 4.2-1: Relationship between limb, illumination condition flags and instrument gain settings

Products parameter	SPH/bright_limb	0 = Dark	1 = Bright	Coming from mission scenario
	SUMMARY_QUALITY/limb_flag	0 = Full Dark 1 = Bright 2 = Twilight	1 = Bright 2 = Twilight	In the geolocation process the sun zenith angle is computed and the occultation then is flagged accordingly
Instrument Gain	SPA Gain	3 (2)	0	Gain setting for spectrometer A. In parenthesis, values valid only for Sirius occultations (starID=1)
	SPB Gain	0	0	Gain setting for spectrometer B

4.3 Thermal Performance

Since the beginning of the mission the hot pixel and RTS phenomena are producing a continuous increase of the dark charge signal within the CCD detectors (see section 4.5.1). In order to minimize this effect, three successive CCD cool down were performed in orbits 800 (25th April 2002), 1050 (13th May 2002) and 2780 (11th September 2002) with a total decrease in temperature of 14 degrees.

Fig. 4.3-1 and 4.3-2 display, respectively, the overall temperature variation and the temperature variation around the Ascending Node Crossing (ANX) time with a resolution of 0.4 degrees (coding accuracy for level 0 data). The CCD temperatures during November are one degree greater than the ones registered during the same period in 2003 (global increase due to the radiator ageing). The expected seasonal variation of the temperatures with amplitude of around one degree can be clearly observed. The peaks that occur mainly in spectrometer B1 and B2 are also to be noted. They happen for some consecutive occultations and every 8-10 days. Their origin is still not known, as we did not find any correlation between these peaks and other activities carried out by other ENVISAT instruments. The CCD temperature at almost the same latitude location (fig. 4.3-2) is monitored in order to detect any inter-orbital temperature variation.

The decrease observed on 24th March 2003, twice in September 2003 and at the beginning of December 2003 in all detectors is after GOMOS switch off periods, when the instrument did not have enough time to reach the nominal temperature before starting the measurements.

The orbital temperature variation of the detector SPB2 (fig. 4.3-3 & 4.3-4) is nominal (around 2.5 degrees). The stability of the temperature during the orbit is important because it affects the position of the interference patterns. The phenomenon of the interference is present mainly in SPB and this Pixel Response Non-Uniformity (PRNU) is corrected during the processing.

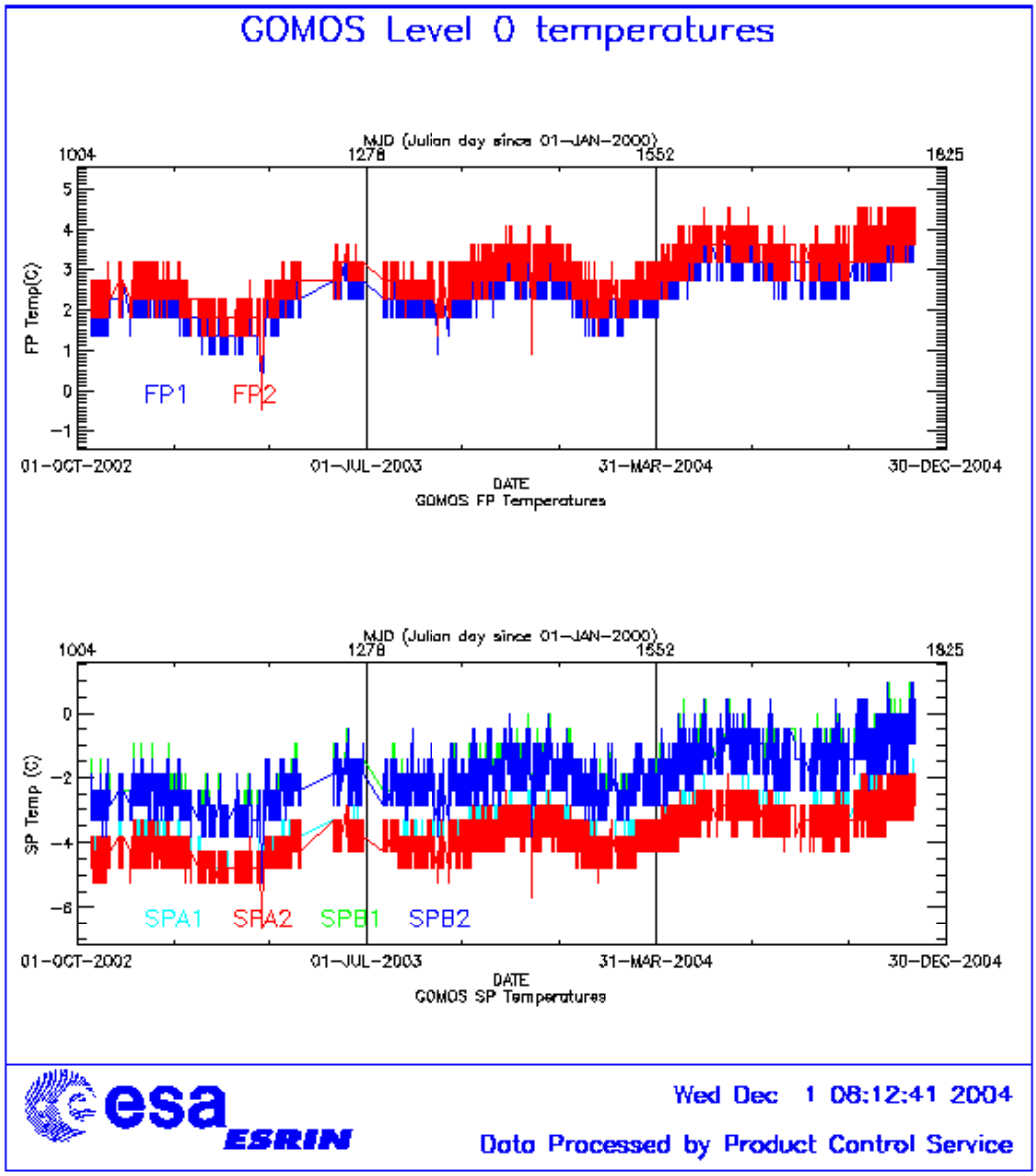

Figure 4.3-1: Level 0 temperature evolution of all GOMOS CCD detectors since October 2002 until the end of the reporting period

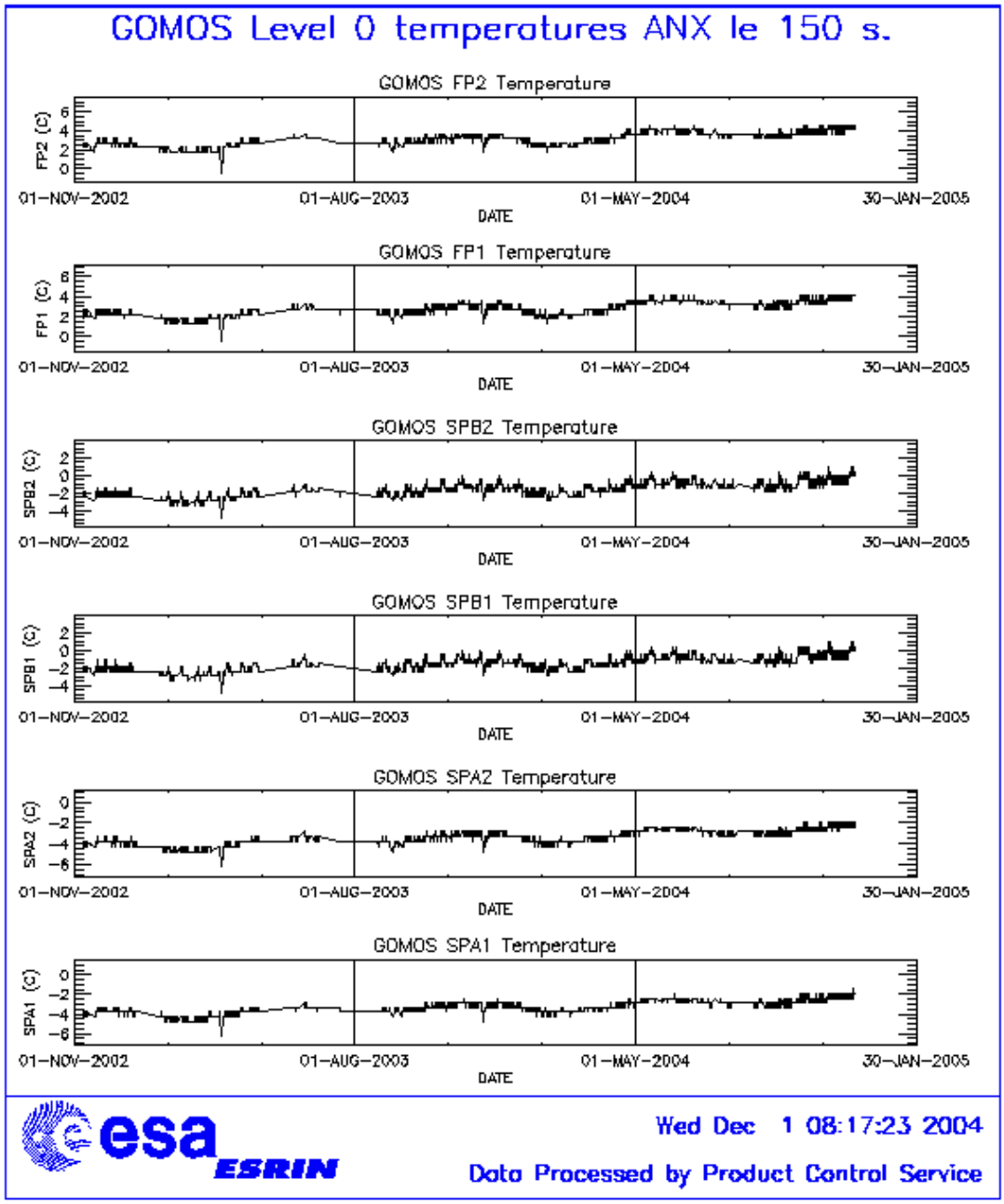

Figure 4.3-2: **Level 0 temperature evolution of all GOMOS CCD detectors around ANX since November 2002 until the end of the reporting period**

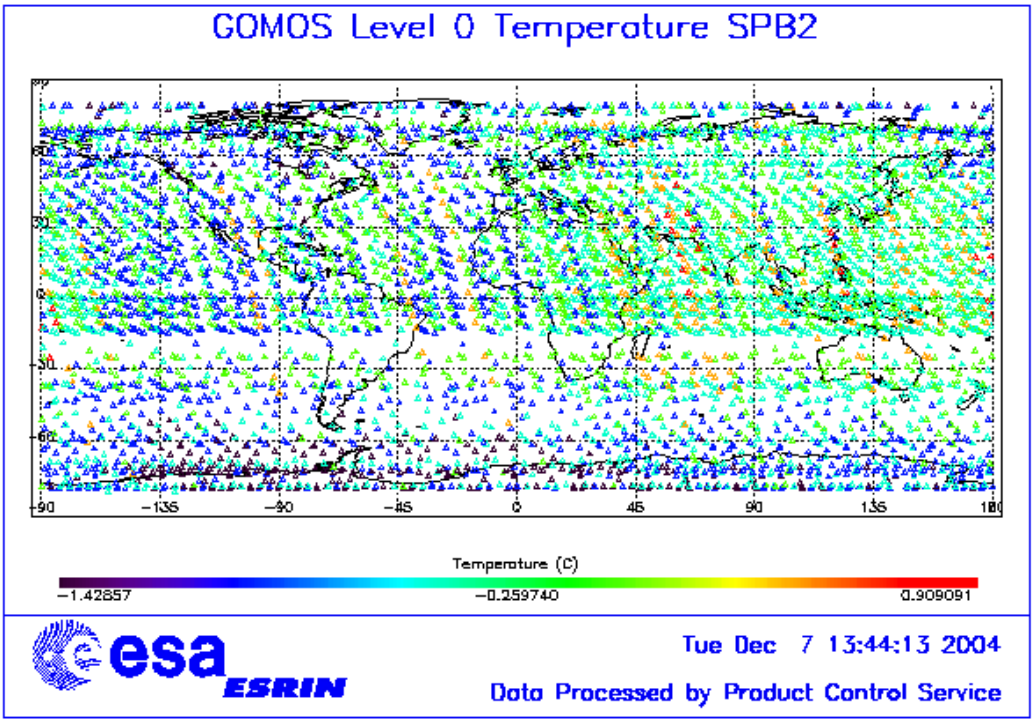

Figure 4.3-3: Ascending orbital variation of SPB2 temperature during reporting period

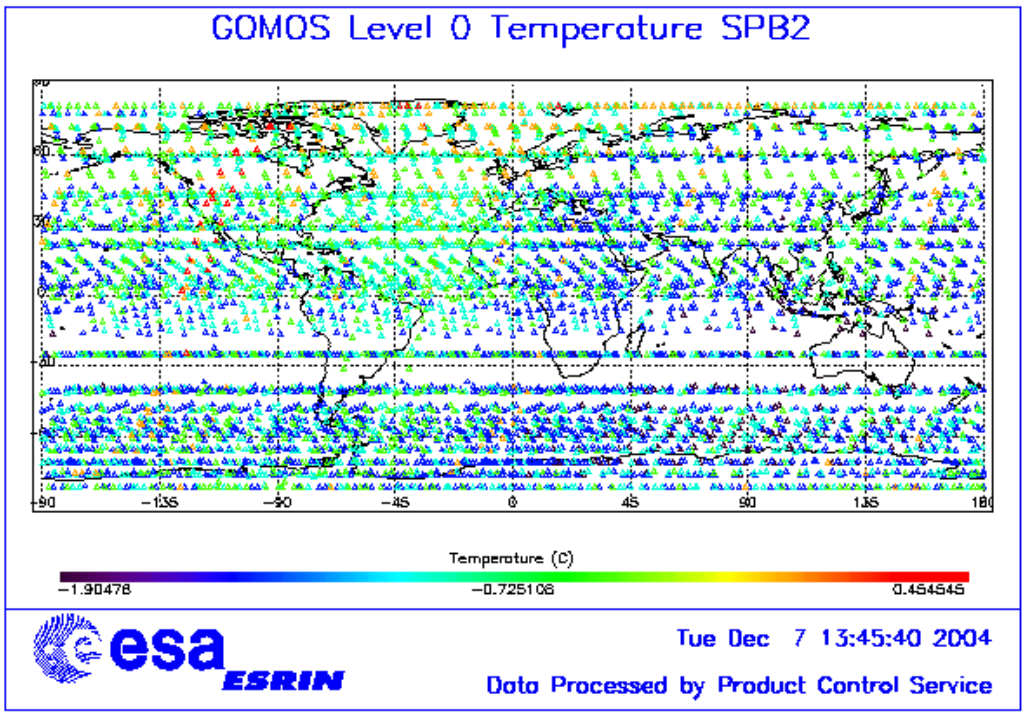

Figure 4.3-4: Descending orbital variation of SPB2 temperature during reporting period

4.4 Optomechanical Performance

No new band setting calibration has been performed during the reporting period. The last one has been done on April.

- Version GOMOS/4.00 and previous ones:

In the processors versions of GOMOS GOMOS/4.00 and previous the spectra is expected to be aligned along CCD lines, and therefore use only a single average line index per CCD. In table 4.4-1 the mean values of the location of the star signal for all the calibration analysis done are reported. The 'left' and 'right' values are calculated (the whole interval is not used) because the spectra present a slight slope, more pronounced in the spectrometer B (see fig. 4-4.1). In table 4.4-2, mean values of the location of the star signal are calculated for some specific wavelength intervals. These intervals have been changed between the calibration performed in September 2002 and the ones performed afterwards (until November 2003). Table 4.4-3 reports the average location of the star spot on the photometer 1 and 2 CCD.

- Version GOMOS/4.02:

In the actual processor version (GOMOS/4.02) operational since 23rd March 2004, a Look Up Table (LUT) gives the line index of the spectra location as a function of the wavelength (blue dots in fig. 4.4-1). A new calibration exercise has been performed during April. The position of the stellar spectra of star id 31, 18 and 4 observed in dark-limb spatial spread monitoring mode have been averaged above 120 km altitude and compared to the values of the LUT. The results confirm the LUT values (see table 4.4-4) so for the time being there is no need to update the LUT.

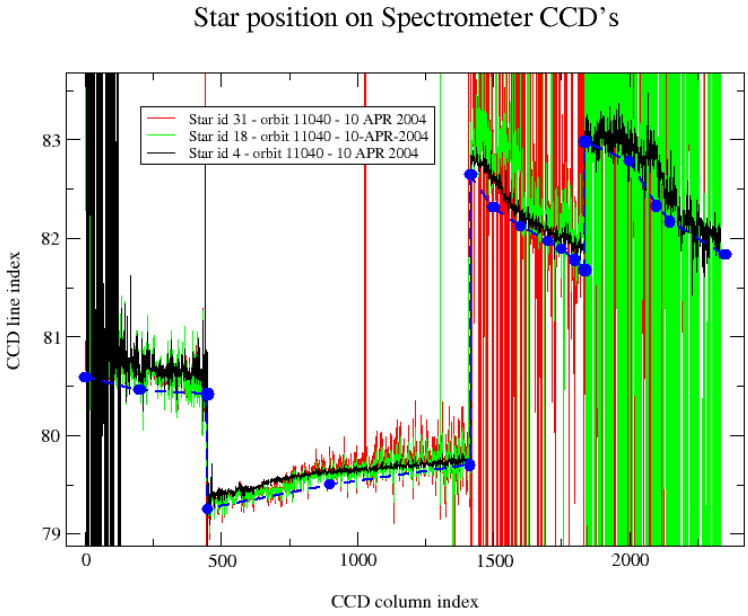

Figure 4.4-1: Average position of star spectra on the CCD

Table 4.4-1: Mean value of the location of the star signal during the occultation at the edges of every band (mean over 50 values, filtering the outliers)

	UV (SPA1) left/right	VIS (SPA2) left/right (Inverted spectra)	IR1 (SPB1) left/right	IR2 (SPB2) left/right
11/09/2002	80.7/80.7	79.8/79.5	82.8/81.9	83.1/82.1
01/01/2003	80.7/80.6	79.8/79.5	82.8/82.0	83.2/82.2
17/07/2003 & 02/08/2003	80.7/80.7	79.8/79.5	82.8/81.9	83.1/82.1
08/11/2003	80.7/80.6	79.8/79.5	82.8/81.9	83.1/82.1

Table 4.4-2: Mean value of the location of the star signal during the occultation (as table 4.4-1) but now within some wavelength intervals

	UV (SPA1)	VIS (SPA2)	IR1 (SPB1)	IR2 (SPB2)
11/09/2002 wl range (nm)	80.8 [300-330]	79.8 [500-530]	82.6 [760-765]	82.9 [937-942]
01/01/2003 wl range (nm)	80.6 [350-360]	78.6 [650-670]	81.6 [760-765]	80.3 [935-945]
02/08/2003	80.6	79.7	82.5	82.8
08/11/2003	80.6	79.9	82.4	82.8

Table 4.4-3: Average column and row pixel location of the star spot on the photometer CCD during the occultation

	FP1 (column/row)	FP2 (column/row)
11/09/2002	11/4	5/5
01/01/2003	10/4	6/4.9
02/08/2003	10/4	6/5
08/11/2003	10/4	6/5

Table 4.4-4: Location of the star signal on the CCD's (corresponding to fig. 4.4-1)

Pixel Column	LUT (Pixel line)	Calibration on 10-APR-2004
0	**80.59**	80.80
20	**80.46**	80.60
449	**80.42**	80.50
450	**79.25**	79.39
900	**79.50**	79.63
1415	**79.70**	79.76
1416	**82.64**	82.80
1500	**82.31**	82.60
1600	**82.12**	82.22
1700	**81.97**	82.04
1750	**81.89**	81.98
1800	**81.78**	81.91
1835	**81.68**	81.88
1836	**82.98**	83.10
2000	**82.78**	82.90
2100	**82.33**	82.70
2150	**82.17**	82.40
2350	**81.83**	82.00

4.5 Electronic Performance

4.5.1 DARK CHARGE EVOLUTION AND TREND

The trend of Dark Charge (DC) is of crucial importance for the final quality of the products, and is therefore subject to intense monitoring. As part of the DC there is:

- "Hot pixels", a pixel is "hot" when its dark charge exceeds its value measured on ground, at the same temperature, by a significant amount.
- RTS phenomenon (Random Telegraphic Signal), it is an abrupt change (positive or negative) of the CCD pixel signal, random in time, affecting only the DC part of the signal and not the photon generated signal.

The temperature dependence of the DC would make this parameter a good indicator of the DC behaviour, but the hot pixels and the RTS are producing a continuous increase of the DC (see trend in fig. 4.5-1 and 4.5-2). To take into account these phenomena, since version GOMOS/4.00 (actual one is GOMOS/4.02) a DC map per orbit is extracted from a Dark Sky Area (DSA) observation performed around ANX (full dark conditions). For every level 1b product (occultation), the actual thermistor temperature of the CCD is used to convert the DC map measured around ANX into an estimate of the DC at the time (and different temperature) of the actual occultation. When the DSA observation is not available, the DC map inside the calibration product that was measured at a given thermistor reference temperature is used; again, the actual thermistor temperature of the CCD is used to compute the actual map. Table 4.5-1 reports the list of products that used the DC maps inside the calibration file due to the non-availability of DSA observation. A "CAL DC map with no T dep." means that, as the temperature information was not available for that occultation, the DC map used is exactly the one inside the Calibration product.

Table 4.5-1: Table of level 1b products that used the Calibration DC maps instead of the DSA observation

Product name	DC information
GOM_TRA_1PNPDE20041101_204954_000000912031_00401_13982_0000.N1	DC map with no T dep.
GOM_TRA_1PNPDE20041101_211759_000000432031_00401_13982_0008.N1	DC map used
GOM_TRA_1PNPDE20041101_211942_000000402031_00401_13982_0009.N1	DC map used
GOM_TRA_1PNPDE20041101_212106_000000402031_00401_13982_0010.N1	DC map used
GOM_TRA_1PNPDE20041101_212328_000000432031_00401_13982_0011.N1	DC map used
GOM_TRA_1PNPDE20041101_212700_000000362031_00401_13982_0012.N1	DC map used
GOM_TRA_1PNPDE20041101_212811_000000372031_00401_13982_0013.N1	DC map used
GOM_TRA_1PNPDE20041101_213048_000000872031_00401_13982_0014.N1	DC map used
GOM_TRA_1PNPDE20041101_213345_000000662031_00401_13982_0015.N1	DC map used
GOM_TRA_1PNPDE20041101_213615_000000392031_00401_13982_0016.N1	DC map used
GOM_TRA_1PNPDE20041101_214008_000000402031_00401_13982_0017.N1	DC map used
GOM_TRA_1PNPDE20041101_214422_000000422031_00401_13982_0018.N1	DC map used
GOM_TRA_1PNPDE20041101_214558_000000562031_00401_13982_0019.N1	DC map used
GOM_TRA_1PNPDE20041101_214942_000000392031_00401_13982_0020.N1	DC map used
GOM_TRA_1PNPDE20041101_215726_000002552031_00401_13982_0021.N1	DC map used
GOM_TRA_1PNPDE20041103_195149_000000462031_00429_14010_0000.N1	DC map used
GOM_TRA_1PNPDE20041103_195513_000000462031_00429_14010_0001.N1	DC map used
GOM_TRA_1PNPDE20041103_200023_000001142031_00429_14010_0002.N1	DC map used

GOM_TRA_1PNPDE20041103_200916_000000572031_00429_14010_0003.N1	DC map used
GOM_TRA_1PNPDE20041103_201244_000000372031_00429_14010_0004.N1	DC map used
GOM_TRA_1PNPDE20041103_201438_000000452031_00429_14010_0005.N1	DC map used
GOM_TRA_1PNPDE20041103_201635_000000372031_00429_14010_0006.N1	DC map used
GOM_TRA_1PNPDE20041103_201802_000000432031_00429_14010_0007.N1	DC map used
GOM_TRA_1PNPDE20041103_202006_000000402031_00429_14010_0008.N1	DC map used
GOM_TRA_1PNPDE20041103_202344_000000422031_00429_14010_0009.N1	DC map used
GOM_TRA_1PNPDE20041103_202635_000000812031_00429_14010_0010.N1	DC map used
GOM_TRA_1PNPDE20041103_202953_000000672031_00429_14010_0011.N1	DC map used
GOM_TRA_1PNPDE20041103_203300_000000392031_00429_14010_0012.N1	DC map used
GOM_TRA_1PNPDE20041103_203656_000000372031_00429_14010_0013.N1	DC map used
GOM_TRA_1PNPDE20041103_204104_000000432031_00429_14010_0014.N1	DC map used
GOM_TRA_1PNPDE20041103_204242_000000412031_00429_14010_0015.N1	DC map used
GOM_TRA_1PNPDE20041103_204411_000000502031_00429_14010_0016.N1	DC map used
GOM_TRA_1PNPDE20041103_204626_000000412031_00429_14010_0017.N1	DC map used
GOM_TRA_1PNPDE20041103_205448_000000632031_00429_14010_0018.N1	DC map used
GOM_TRA_1PNPDE20041106_011126_000000402031_00460_14041_0001.N1	DC map used
GOM_TRA_1PNPDE20041106_011258_000000402031_00460_14041_0002.N1	DC map used
GOM_TRA_1PNPDE20041106_195422_000000942031_00472_14053_0000.N1	DC map used
GOM_TRA_1PNPDE20041106_195739_000000472031_00472_14053_0001.N1	DC map used
GOM_TRA_1PNPDE20041106_200111_000000422031_00472_14053_0002.N1	DC map used
GOM_TRA_1PNPDE20041106_200436_000000862031_00472_14053_0003.N1	DC map used
GOM_TRA_1PNPDE20041106_200903_000000472031_00472_14053_0004.N1	DC map used
GOM_TRA_1PNPDE20041106_201248_000001402031_00472_14053_0005.N1	DC map used
GOM_TRA_1PNPDE20041106_201925_000000412031_00472_14053_0006.N1	DC map used
GOM_TRA_1PNPDE20041106_202232_000000392031_00472_14053_0007.N1	DC map used
GOM_TRA_1PNPDE20041106_202543_000000412031_00472_14053_0008.N1	DC map used
GOM_TRA_1PNPDE20041106_202934_000000382031_00472_14053_0009.N1	DC map used
GOM_TRA_1PNPDE20041106_203440_000000662031_00472_14053_0010.N1	DC map used
GOM_TRA_1PNPDE20041106_203845_000000392031_00472_14053_0011.N1	DC map used
GOM_TRA_1PNPDE20041106_204249_000000392031_00472_14053_0012.N1	DC map used
GOM_TRA_1PNPDE20041106_204644_000000432031_00472_14053_0013.N1	DC map used
GOM_TRA_1PNPDE20041106_204822_000000412031_00472_14053_0014.N1	DC map used
GOM_TRA_1PNPDE20041106_205004_000000522031_00472_14053_0015.N1	DC map used
GOM_TRA_1PNPDE20041106_205211_000000422031_00472_14053_0016.N1	DC map used
GOM_TRA_1PNPDE20041110_211229_000000482032_00029_14111_0000.N1	DC map used
GOM_TRA_1PNPDE20041110_211609_000000422032_00029_14111_0001.N1	DC map used
GOM_TRA_1PNPDE20041110_212114_000000812032_00029_14111_0002.N1	DC map used
GOM_TRA_1PNPDE20041110_212340_000000532032_00029_14111_0003.N1	DC map used
GOM_TRA_1PNPDE20041110_212649_000001032032_00029_14111_0004.N1	DC map used
GOM_TRA_1PNPDE20041110_212940_000001262032_00029_14111_0005.N1	DC map used
GOM_TRA_1PNPDE20041110_213406_000000392032_00029_14111_0006.N1	DC map used
GOM_TRA_1PNPDE20041110_213812_000000402032_00029_14111_0007.N1	DC map used
GOM_TRA_1PNPDE20041110_214016_000000422032_00029_14111_0008.N1	DC map used
GOM_TRA_1PNPDE20041110_214214_000000472032_00029_14111_0009.N1	DC map used
GOM_TRA_1PNPDE20041110_214811_000000602032_00029_14111_0010.N1	DC map used
GOM_TRA_1PNPDE20041110_215326_000000402032_00029_14111_0011.N1	DC map used
GOM_TRA_1PNPDE20041110_215739_000000352032_00029_14111_0012.N1	DC map used
GOM_TRA_1PNPDE20041110_220117_000000472032_00029_14111_0013.N1	DC map used
GOM_TRA_1PNPDE20041110_220256_000000442032_00029_14111_0014.N1	DC map used

GOM_TRA_1PNPDE20041110_220453_000000402032_00029_14111_0015.N1	DC map used
GOM_TRA_1PNPDE20041110_220652_000000482032_00029_14111_0016.N1	DC map used
GOM_TRA_1PNPDE20041110_220823_000000402032_00029_14111_0017.N1	DC map used
GOM_TRA_1PNPDE20041110_221614_000000792032_00029_14111_0018.N1	DC map used
GOM_TRA_1PNPDE20041114_214056_000000462032_00086_14168_0022.N1	DC map used
GOM_TRA_1PNPDE20041114_214240_000000382032_00086_14168_0023.N1	DC map used
GOM_TRA_1PNPDE20041114_214717_000000362032_00086_14168_0024.N1	DC map used
GOM_TRA_1PNPDE20041114_214929_000000492032_00086_14168_0025.N1	DC map used
GOM_TRA_1PNPDE20041114_215110_000000952032_00086_14168_0026.N1	DC map used
GOM_TRA_1PNPDE20041114_215413_000000372032_00086_14168_0027.N1	DC map used
GOM_TRA_1PNPDE20041115_201228_000000802032_00100_14182_0000.N1	DC map with no T dep.
GOM_TRA_1PNPDE20041115_201443_000000822032_00100_14182_0001.N1	DC map used
GOM_TRA_1PNPDE20041115_201659_000000562032_00100_14182_0002.N1	DC map used
GOM_TRA_1PNPDE20041115_201858_000000402032_00100_14182_0003.N1	DC map used
GOM_TRA_1PNPDE20041115_202359_000000732032_00100_14182_0004.N1	DC map used
GOM_TRA_1PNPDE20041115_202617_000000542032_00100_14182_0005.N1	DC map used
GOM_TRA_1PNPDE20041115_202849_000000932032_00100_14182_0006.N1	DC map used
GOM_TRA_1PNPDE20041115_203150_000000502032_00100_14182_0007.N1	DC map used
GOM_TRA_1PNPDE20041115_203640_000000382032_00100_14182_0008.N1	DC map used
GOM_TRA_1PNPDE20041115_203850_000000452032_00100_14182_0009.N1	DC map used
GOM_TRA_1PNPDE20041115_204040_000000382032_00100_14182_0010.N1	DC map used
GOM_TRA_1PNPDE20041115_204244_000000412032_00100_14182_0011.N1	DC map used
GOM_TRA_1PNPDE20041115_204549_000000422032_00100_14182_0012.N1	DC map used
GOM_TRA_1PNPDE20041115_204747_000000362032_00100_14182_0013.N1	DC map used
GOM_TRA_1PNPDE20041115_204924_000000572032_00100_14182_0014.N1	DC map used
GOM_TRA_1PNPDE20041115_205224_000000632032_00100_14182_0015.N1	DC map used
GOM_TRA_1PNPDE20041115_205558_000000382032_00100_14182_0016.N1	DC map used
GOM_TRA_1PNPDE20041115_210215_000000392032_00100_14182_0018.N1	DC map used
GOM_TRA_1PNPDE20041115_210514_000000432032_00100_14182_0019.N1	DC map used
GOM_TRA_1PNPDE20041115_210737_000000382032_00100_14182_0020.N1	DC map used
GOM_TRA_1PNPDE20041115_210918_000000472032_00100_14182_0021.N1	DC map used
GOM_TRA_1PNPDE20041115_211106_000000372032_00100_14182_0022.N1	DC map used
GOM_TRA_1PNPDE20041115_211544_000000342032_00100_14182_0023.N1	DC map used
GOM_TRA_1PNPDE20041115_211758_000000492032_00100_14182_0024.N1	DC map used
GOM_TRA_1PNPDE20041115_211948_000001032032_00100_14182_0025.N1	DC map used
GOM_TRA_1PNPDE20041115_212441_000000772032_00100_14182_0026.N1	DC map used
GOM_TRA_1PNPDE20041116_194323_000000832032_00114_14196_0000.N1	DC map used
GOM_TRA_1PNPDE20041116_194725_000000392032_00114_14196_0001.N1	DC map used
GOM_TRA_1PNPDE20041116_195140_000001052032_00114_14196_0002.N1	DC map used
GOM_TRA_1PNPDE20041116_195441_000000542032_00114_14196_0003.N1	DC map used
GOM_TRA_1PNPDE20041116_195708_000000842032_00114_14196_0004.N1	DC map used
GOM_TRA_1PNPDE20041116_201408_000000402032_00114_14196_0010.N1	DC map used
GOM_TRA_1PNPDE20041116_201612_000000372032_00114_14196_0011.N1	DC map used
GOM_TRA_1PNPDE20041128_200000_000000542032_00286_14368_0000.N1	DC map with no T dep.
GOM_TRA_1PNPDE20041128_200140_000000582032_00286_14368_0001.N1	DC map used
GOM_TRA_1PNPDE20041128_200332_000000582032_00286_14368_0002.N1	DC map used
GOM_TRA_1PNPDE20041128_200514_000000762032_00286_14368_0003.N1	DC map used
GOM_TRA_1PNPDE20041128_200904_000000742032_00286_14368_0004.N1	DC map used
GOM_TRA_1PNPDE20041128_201117_000000802032_00286_14368_0005.N1	DC map used
GOM_TRA_1PNPDE20041128_201545_000001162032_00286_14368_0006.N1	DC map used

GOM_TRA_1PNPDE20041128_201934_000000662032_00286_14368_0007.N1	DC map used
GOM_TRA_1PNPDE20041128_202244_000000732032_00286_14368_0008.N1	DC map used
GOM_TRA_1PNPDE20041128_202531_000000652032_00286_14368_0009.N1	DC map used
GOM_TRA_1PNPDE20041128_202741_000000572032_00286_14368_0010.N1	DC map used
GOM_TRA_1PNPDE20041128_202913_000000402032_00286_14368_0011.N1	DC map used
GOM_TRA_1PNPDE20041128_203137_000000402032_00286_14368_0012.N1	DC map used
GOM_TRA_1PNPDE20041128_203346_000000392032_00286_14368_0013.N1	DC map used
GOM_TRA_1PNPDE20041128_203932_000000372032_00286_14368_0014.N1	DC map used
GOM_TRA_1PNPDE20041128_204721_000000382032_00286_14368_0015.N1	DC map used
GOM_TRA_1PNPDE20041128_205200_000000382032_00286_14368_0016.N1	DC map used
GOM_TRA_1PNPDE20041129_193349_000000682032_00300_14382_0000.N1	DC map used
GOM_TRA_1PNPDE20041129_193739_000000732032_00300_14382_0001.N1	DC map used
GOM_TRA_1PNPDE20041129_193949_000000772032_00300_14382_0002.N1	DC map used
GOM_TRA_1PNPDE20041129_194410_000001072032_00300_14382_0003.N1	DC map used
GOM_TRA_1PNPDE20041129_194753_000000652032_00300_14382_0004.N1	DC map used
GOM_TRA_1PNPDE20041129_195100_000000682032_00300_14382_0005.N1	DC map used
GOM_TRA_1PNPDE20041129_195343_000000642032_00300_14382_0006.N1	DC map used
GOM_TRA_1PNPDE20041129_195558_000000562032_00300_14382_0007.N1	DC map used
GOM_TRA_1PNPDE20041129_195733_000000392032_00300_14382_0008.N1	DC map used
GOM_TRA_1PNPDE20041129_195956_000000402032_00300_14382_0009.N1	DC map used
GOM_TRA_1PNPDE20041129_200208_000000372032_00300_14382_0010.N1	DC map used
GOM_TRA_1PNPDE20041129_200422_000000392032_00300_14382_0011.N1	DC map used
GOM_TRA_1PNPDE20041129_200540_000000382032_00300_14382_0012.N1	DC map used
GOM_TRA_1PNPDE20041129_200757_000000402032_00300_14382_0013.N1	DC map used
GOM_TRA_1PNPDE20041129_201543_000000382032_00300_14382_0014.N1	DC map used
GOM_TRA_1PNPDE20041129_202023_000000392032_00300_14382_0015.N1	DC map used
GOM_TRA_1PNPDE20041129_202227_000000472032_00300_14382_0016.N1	DC map used
GOM_TRA_1PNPDE20041129_202401_000000522032_00300_14382_0017.N1	DC map used
GOM_TRA_1PNPDE20041129_202537_000000412032_00300_14382_0018.N1	DC map used
GOM_TRA_1PNPDE20041129_202739_000000392032_00300_14382_0019.N1	DC map used
GOM_TRA_1PNPDE20041129_203033_000000372032_00300_14382_0020.N1	DC map used
GOM_TRA_1PNPDE20041129_203334_000000362032_00300_14382_0021.N1	DC map used

In fig. 4.5-1 and 4.5-2 it is plotted the average DC inserted by the processor into the level 1b data products for the spectrometers SPA1 and SPB2 (per band: upper, central and lower). From the figures, it can be seen that the DC is increasing at the expected rate.

The same DC values are plotted in fig. 4.5-3 but for some occultations belonging only to the reporting month.

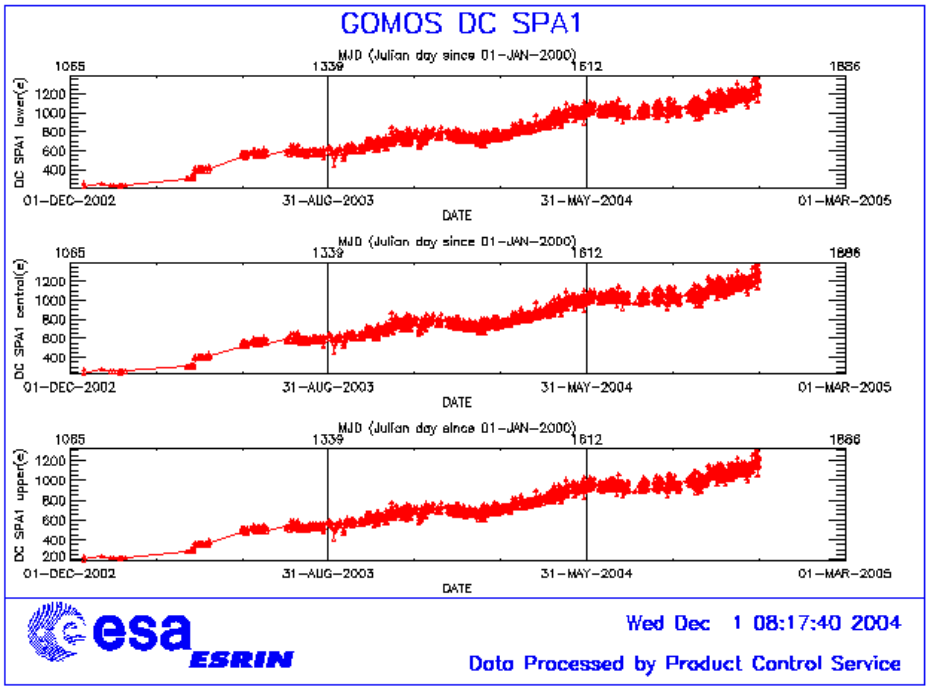

Figure 4.5-1: Mean DC evolution on SPA1 since 15th December 2002 until the end of the reporting period

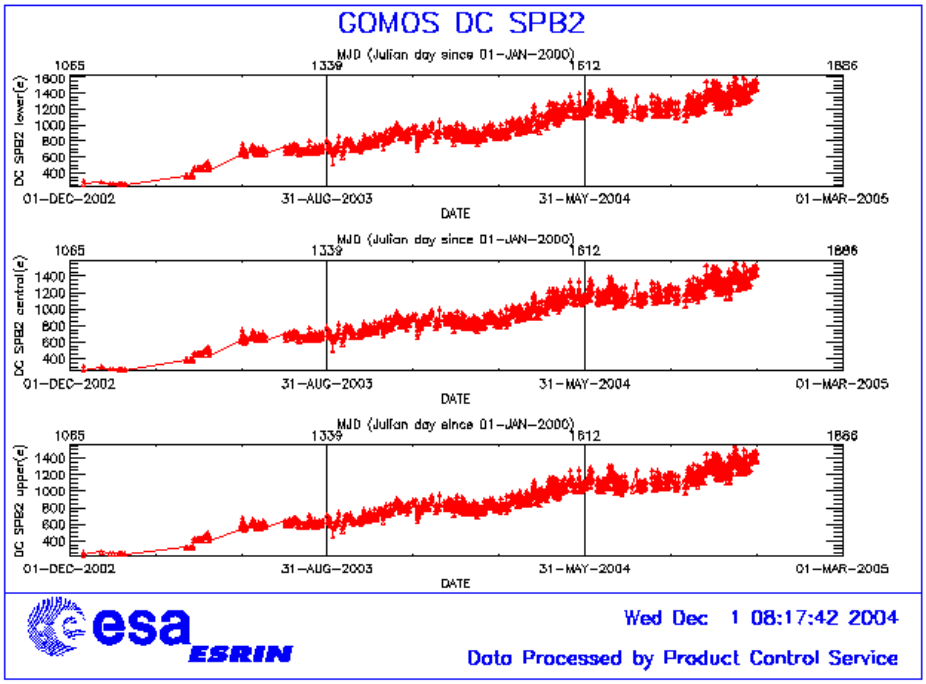

Figure 4.5-2: Mean DC evolution on SPB2 from 15th December 2002 until the end of the reporting period

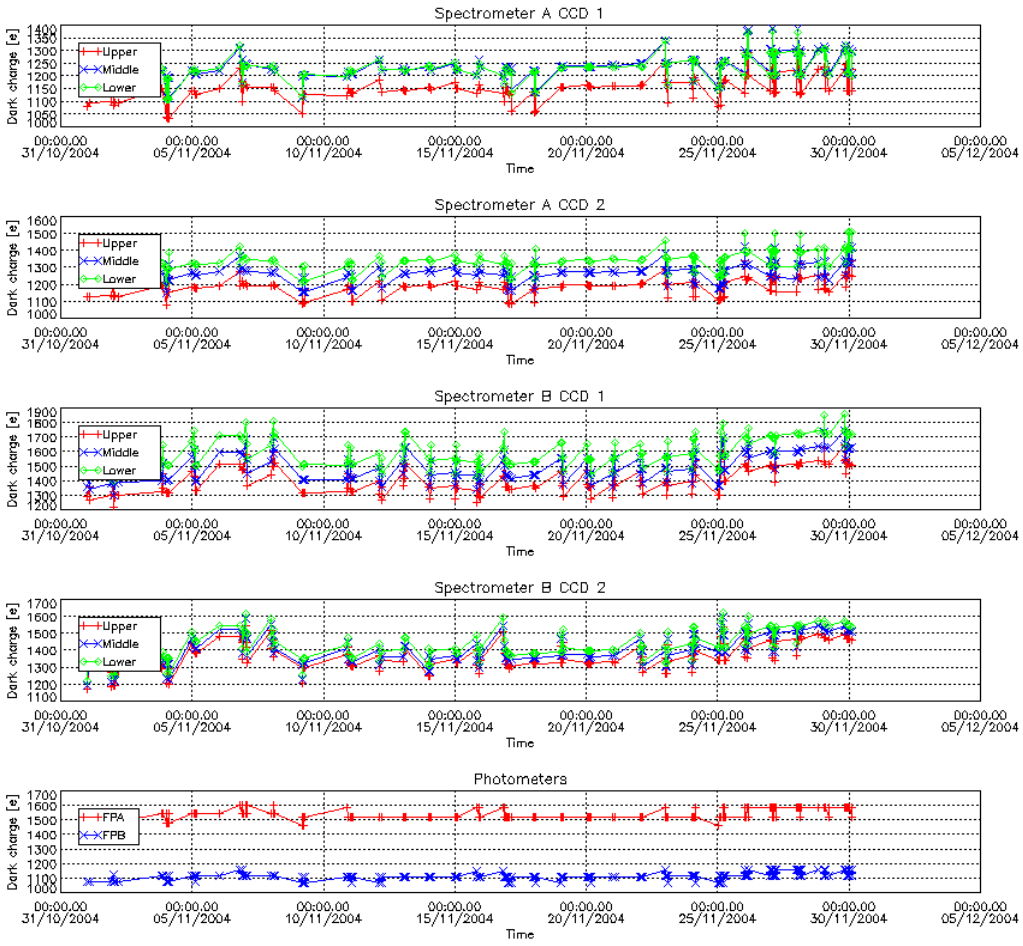

Figure 4.5-3: Mean Dark Charge of spectrometers and photometers during reporting period

4.5.2 SIGNAL MODULATION

A parasitic signal was found to be systematically present, added to the useful signal, at least for spectrometers A1 and A2. The modulation is corrected in the data processing, but the modulation signal standard deviation is routinely monitored in order to detect any trend (fig. 4.5-4).

The modulation standard deviation, for every spectrometer, is characterised as follows:

$$\sigma_{mod} = (\text{'static noises'} - \text{'total static variance'})^{1/2} / \text{gain} \qquad \text{(in ADU)}$$

- The 'static noises' are calculated from the DSA observation performed once per orbit
- The 'total static variance' is obtained from ADF data (electronic chain noise, quantization noise).

The standard deviation of the modulation signal (fig. 4.5-4) presents high values after the inclusion, at the end of March 2004, of the ESRIN level 0 data. It is now confirmed that the South Atlantic Anomaly is

the cause of these unexpected peaks. The quality of ESRIN data, in particular over the SAA zone, is thus under investigation. However, in the second half of October the peaks are smaller because the DSA zone where the data are taking for this analysis is moving towards the Northern Hemisphere. At the end of October the DSA zone is definitely chosen by the planning system in the Northern Hemisphere (to fill the criteria 'DSA in full dark limb conditions') and the high peaks disappear.

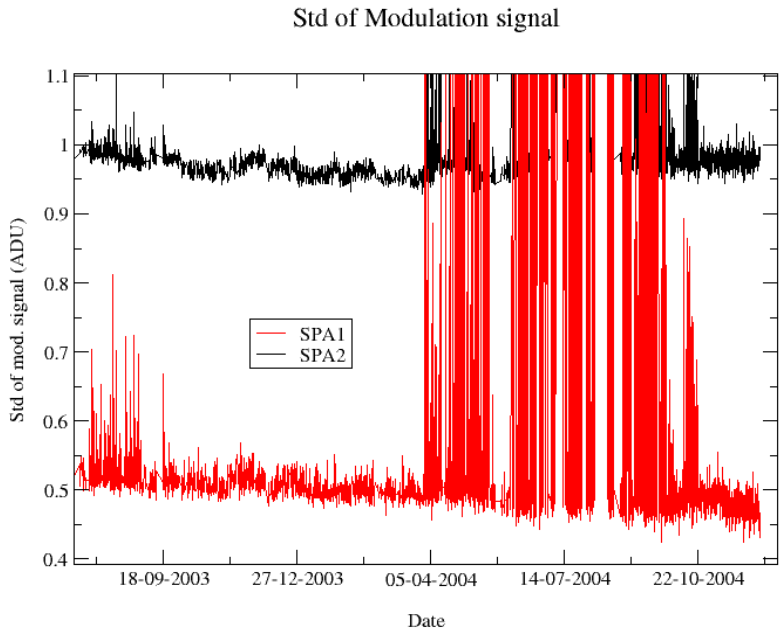

Figure 4.5-4: Standard deviation of the modulation signal

4.5.3 ELECTRONIC CHAIN GAIN AND OFFSET

No new electronic chain gain and offset calibration has been done during the reporting period so these results have been already presented in previous MR.

The routine monitoring of the ADC offset is a good indicator of the ageing of the instrument electronics. During the definition of this routine activity, an exercise has been done to analyze the variation of the ADC offset using the calibration observation in linearity mode (orbits 2810, 4384, 4834, 5219 and 5734). The fig. 4.5-5 presents the evolution of the calibrated ADC offset for each spectrometer electronic chain. The unexpected increase of this offset seems to be due to an external contribution. In the ADC offset calibration procedure, linearity observations are used with two integration times of 0.25 and 0.50 seconds to extrapolate to an integration time of 0 seconds that give the complete chain offset and not only the ADC offset. The complete offset contains any possible offsets, and especially the static dark charge (i.e. the dark charge that does not depend on the spectrometer integration time). If the memory area of the CCD is affected by the generation of hot pixels (this is confirmed by the presence of vertical lines visible in the measurement maps in spatial spread monitoring mode), it becomes that the increase observed in fig. 4.5-5 is due to these new hot pixels.

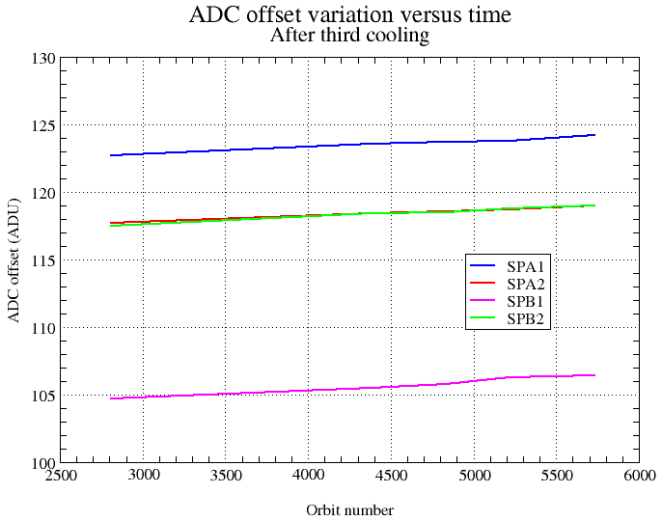

Figure 4.5-5: Evolution of the ADC offset for each spectrometer electronic chain

Next task consists in completing the analysis to confirm that the offset increase is due to the hot pixels in memory area. This can be proven by the study of the noise due to the increased dark charge. The increase of ADC offset will be assumed to be equal to the increase of 'static dark charge' and the corresponding noise will be computed and compared to the increase of the signal variance residual.

If we keep the ADC offset constant, as it is also used to compute the dark charge at band level used to correct the samples in the level 1b processing, the increase of the static dark charge - not taken into account in the ADC offset - is compensated by an artificial increase of the calibrated dark charge. So, the star and limb spectra are correctly corrected for dark charge. A small bias can be added to the instrument noise due to the incorrect dark charge level. Anyway, this quantity is not large enough to require a modification of the ADC offset value.

4.6 Acquisition, Detection and Pointing Performance

4.6.1 SATU NOISE EQUIVALENT ANGLE

The Star Acquisition and Tracking Unit (SATU) noise equivalent angle (SATU NEA) consists of the statistical angular variation of the SATU data above the atmosphere.
The mean of the standard deviation (STD over the 50 values per measurement) above 105 km are computed for every occultation, giving two values per occultation: one in the 'X' direction, one in the 'Y' direction. A mean value per day in every direction and limb is calculated and monitored in order to assess instrument performance in terms of star pointing. The thresholds are 2 and 3 micro radians in 'X' and 'Y' directions respectively. Before May 2003, data above 90 km have been considered (instead of 105 km) but from May 2003 on, data taken in the mesospheric oxygen layer (located around 100 km altitude) have been avoided because they could cause fluctuations on the SATU data. Also the products with errors (error flag set) are discarded from May 2003 onwards.

It can be seen in fig. 4-6.1 that the SATU NEA had some increase for 'Y' direction but still well below the threshold.

The results for some occultations belonging also to previous months (monthly averages) are presented in fig. 4.6-2 where a small increase is noted mainly for 'Y' direction. This trend could be a local trend and is to be confirmed during the following months.

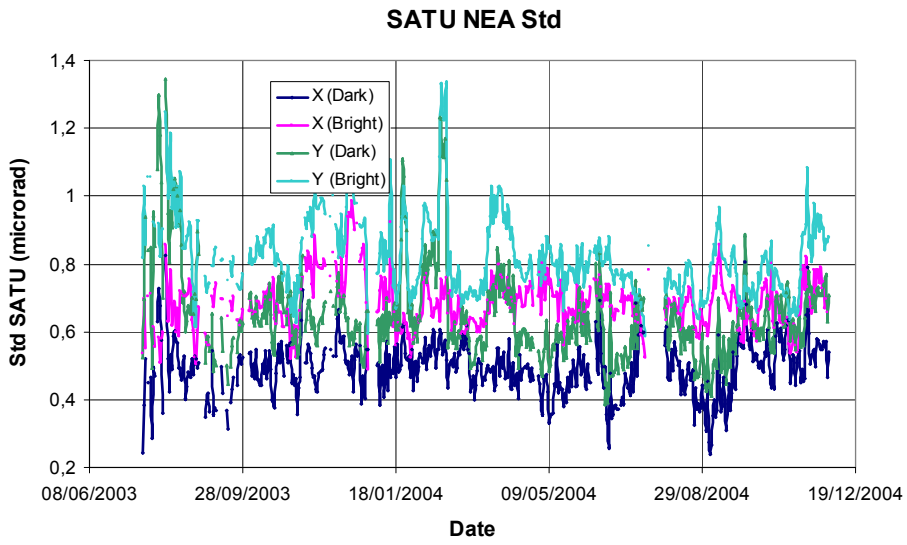

Thresholds:
'X' direction: 2 microrad
'Y' direction: 3 microrad

Figure 4.6-1: Average value per day of SATU NEA STD above 105 km

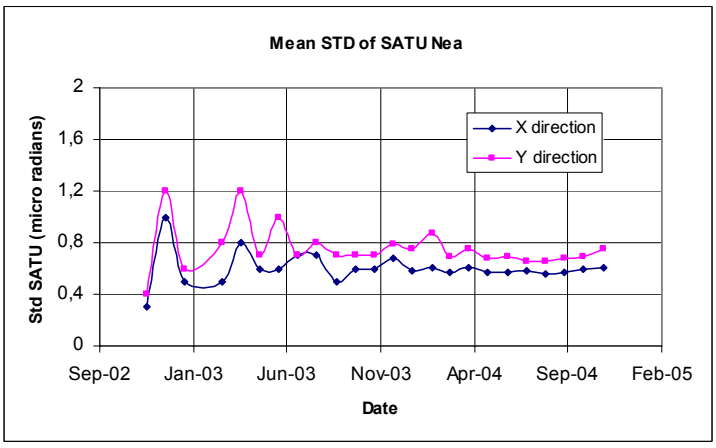

Figure 4.6-2: Average value per month of SATU NEA STD above 105 km

4.6.2 TRACKING LOSS INFORMATION

This verification consists of the monitoring of the tangent altitude at which the star is lost. It is an indicator of the pointing performance although it is to be considered that star tracking is also lost due to the presence of clouds and hence not only due to deficiencies in the pointing performance. Therefore,

only the detection of any systematic long-term trend is the main purpose of this monitoring. The recent results are presented in fig. 4.6-3, 4.6-4 and 4.6-5:

- The dependence of the altitude at which tracking is lost on the magnitude of the star is very small because the tracking is mainly lost due to the refraction and the scintillation that depend on the atmospheric conditions.
- There are three stars lost at very high altitude in dark limb (fig. 4.6-3). They are long lasting occultations so the fact that the star is lost at a very high altitude is not related to deficiencies in pointing.
- In bright limb, the star lost at around 40 km altitude (fig. 4.6-4) is a partial occultation (at the end of the orbit). The entire occultation is included within the following orbit; so again, this is not related to poor pointing performances. The star lost at 50 km is due to the failures in the acquisition chain between 12-16 November, but the reprocessed data is OK.
- In twilight limb (fig. 4.6-5), the stars lost at high altitude correspond to partial occultations or to long lasting occultations.
- Some daily statistics are given in fig. 4.6-6 for dark and bright limb occultations. The high peaks are due to the long lasting occultations or partial occultations. No trend is detected for the reporting period.
- Some monthly statistics are given in fig. 4.6-7 calculated for a set of data and not for the whole months. For the moment, no trend is visible in the plot.

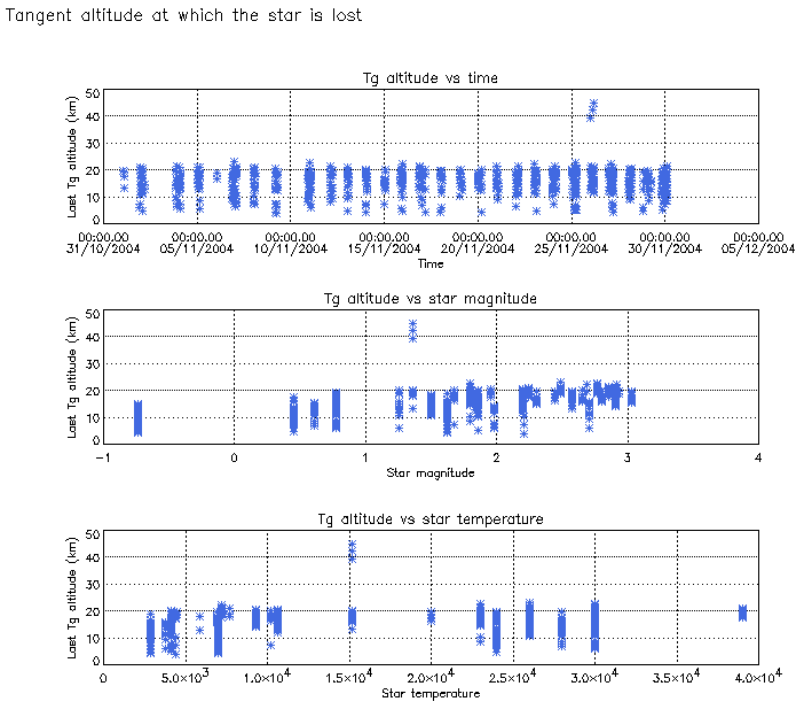

Figure 4.6-3: Last tangent altitude of the occultation (dark limb), point at which the star is lost

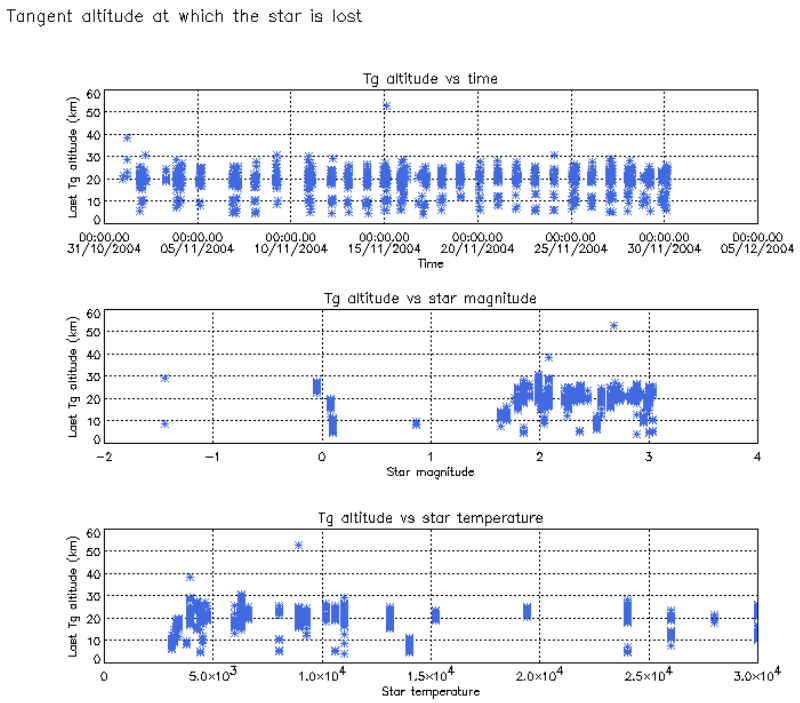

Figure 4.6-4: Last tangent altitude of the occultation (bright limb), point at which the star is lost

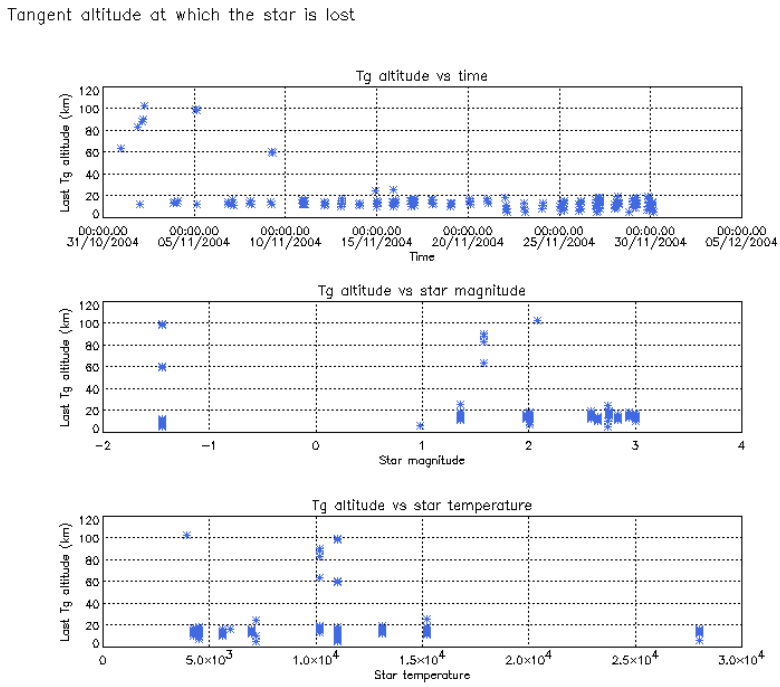

Figure 4.6-5: Last tangent altitude of the occultation (twilight limb), point at which the star is lost

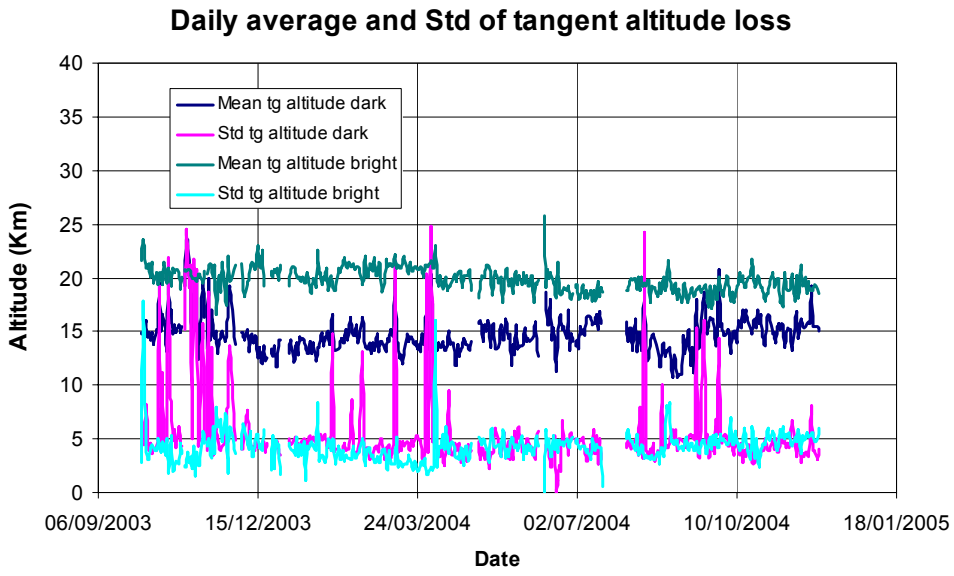

Figure 4.6-6: Daily average and STD of tangent altitude loss for the reporting period

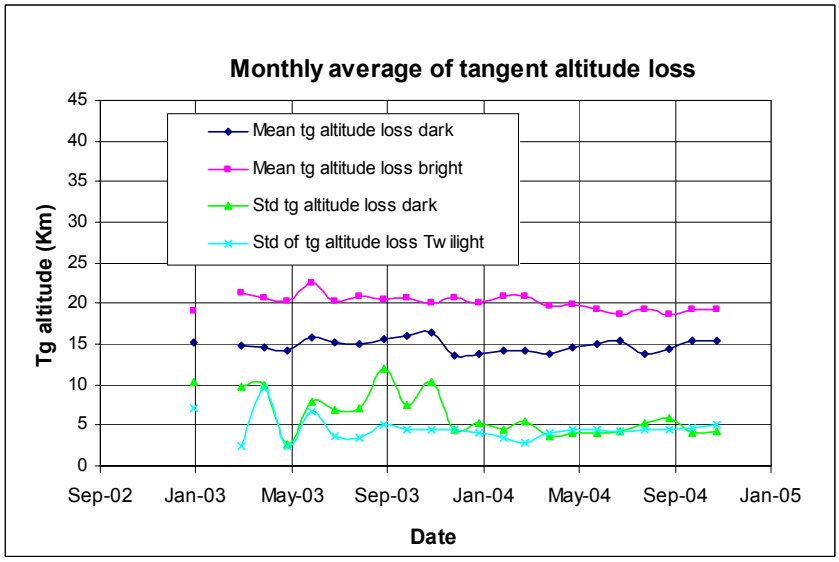

Figure 4.6-7: Monthly mean tangent altitude (and STD) at which the star is lost since January 2003

4.6.3 MOST ILLUMINATED PIXEL (MIP)

The MIP (Most Illuminated Pixel) is the star position on the SATU CCD in detection mode and it is recorded in the housekeeping data. The nominal centre of the SATU is pixel number **145** in elevation and number **205** in azimuth. The detection of the stars should not be far from this centre. As can be seen in fig. 4.6-8 the azimuth is always well within the threshold (table 4.6-1) since September 2002 even if a

small variation is present. The elevation MIP has a significant variation (see the *note* below) till 12th December 2003 when a new PSO algorithm was activated in order to reduce the deviations of the ENVISAT platform attitude with respect to the nominal one. The annual amplitude of the MIP displacement is decreased from 18-20 pixels to 8-10 that means an important improvement of the ENVISAT pointing performance. This result confirms that, until now, the algorithm is working as expected.

From orbit 14132 until orbit 14200 and in coincidence with the period of acquisition failures of 12-16 November (see fig. 4.6-8 and zoom) a gradual increase in elevation corresponding to a total mispointing of 20 mdeg is observed. This local increase has no impact on the operations of GOMOS.

Table 4.6-1: MIP Thresholds

MIP X	**Mean delta Az**	[198 - 210]
	Std delta Az	7
MIP Y	**Mean delta El**	[140 – 150]
	Std delta El	4

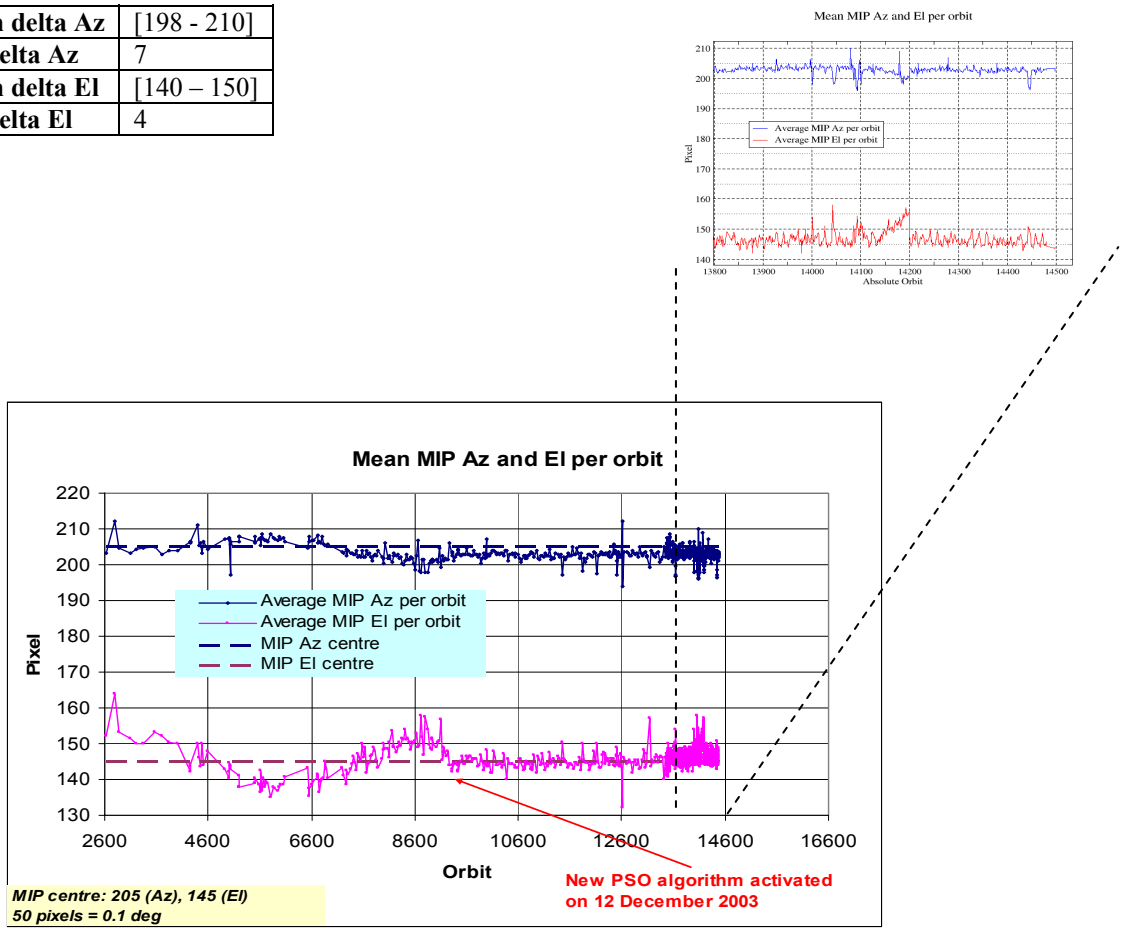

Figure 4.6-8: Mean values of MIP for some orbits since 1st September 2002 (see table 4.5-1)

Note: A MIP variation onto the SATU CCD of 50 pixels corresponds to a de-pointing of 0.1 degrees

Fig. 4.6-9 shows the standard deviation of azimuth and elevation that should be within the thresholds of table 4.6-1. The peaks observed mean that one (or more) star/s where detected very far from the SATU

centre and, in this case, the star/s is lost during the centering phase (see section 3.2 for stars lost in centering).

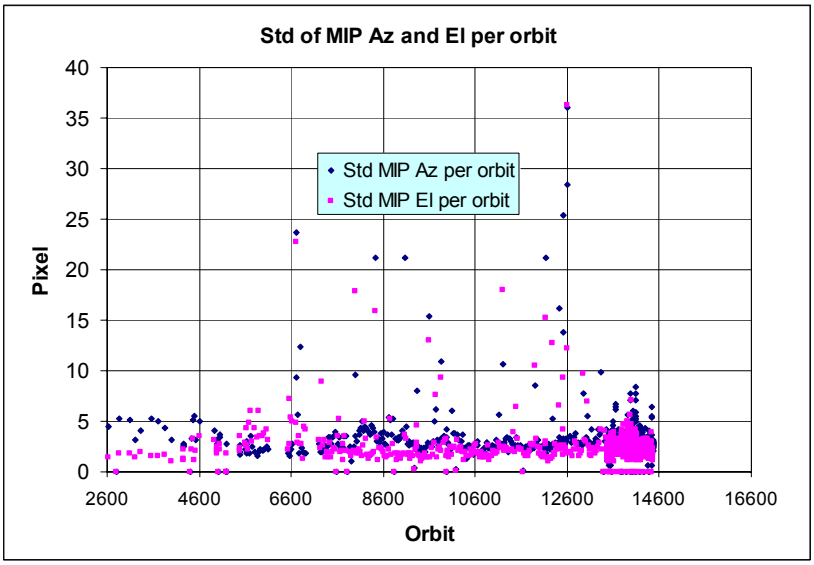

Figure 4.6-9: Standard deviation of MIP Azimuth and Elevation for some orbits since 1st September 2002 until end of reporting period (see table 4.6-1)

5 LEVEL 1 PRODUCT QUALITY MONITORING

5.1 Processor Configuration

5.1.1 VERSION

About 16% of GOM_TRA_1P products have been received in the PCF for routine quality control and long term trend quality monitoring. The current level 1-processor software version for the operational ground segment is GOMOS/4.02 (see table 5.1-1). The product specification is PO-RS-MDA-GS2009_10_3H. This processor has been cleared for initial level 1 data release, with a disclaimer for known artefacts (http://envisat.esa.int/dataproducts/availability/disclaimers) that are currently being resolved and will be implemented in the next release (http://envisat.esa.int/dataproducts/availability).

Cal/Val teams are supplied with selected data sets generated by the prototype processor GOPR 6.0a. See table 5.1-2 for prototype level 1b versions and modifications.

Table 5.1-1: PDS level 1b product version and main modifications implemented

Date	Version	Description of changes
23-MAR-2004	Level 1b version 4.02 at PDHS-E and PDHS-K	Algorithm baseline level 1b DPM 6.0 • Adding a new calibration parameters (these values are hard coded at the moment) • Removal of redundancy chain from code • Modifications in the processing to apply new configuration and calibration parameter

		• New algorithm to determine between dark, twilight and bright limb and to handle data accordingly • Added handling of source packages with invalid packet header • Added enumerations for all configuration flags • See ref. [2] for more details
31-MAY-2003	Level 1b version 4.00 at PDHS-E and PDHS-K	Algorithm baseline level 1b DPM 5.4: • Modulation correction step added after the cosmic rays detection processing • Inversion of the non-linearity and offset corrections • Modification of the computation of the estimated background signal measured by the photometers: use the spectrometer radiometric sensitivity curve and the photometer transfer function. • Use of the dark charge map at orbit level computed from the DSA (dark sky area) if any in the level 0 product • Implementation of a new unfolding algorithm for the photometer samples • See ref. [2] for more details
21-NOV-2002	Level 1b version 3.61 at PDHS-E and PDHS-K	Algorithm baseline DPM 5.3: • Review of some default values • New definition of one PCD flag (atmosphere) • Temporal interpolation of ECMWF data • See ref. [2] for more details

Table 5.1-2: GOPR level 1b product version and main modifications implemented

Date	Version	Description of changes
17-MAR-2004	GOPR 6.0a	• Provide SFA and SATU angles in degrees • Elevation angle dependency of the reflectivity LUT added in the algorithms • Ratio upper/star signal added (FLAGUC) • Add Dark Charge used for dark charge correction (per band) • Flag for illumination condition (PCDillum) • Minimum sample value for which the cosmic rays detection processing is applied (Crmin) is a function of gain index • Logic for computation of the flags attached to the reference star spectrum (Flref) modified • Add the computation of the sun direction in the inertial geocentric frame to be written in the level 1b and limb products. • Spectrometer effective sampling time added (To be completed)
25-JUL-2003	GOPR 5.4f	• The demodulation process is applied only in full dark limb and twilight limb conditions.
17-JUL-2003	GOPR 5.4e	• Sun zenith angle is computed in the geolocation process. The occultation is now classified into full dark limb condition, (1) bright limb condition and (2) twilight limb condition. • No background correction applied in full dark limb condition. The location of the image of the star spectrum on the CCD array is no more aligned with the CCD lines.
02-JUL2003	GOPR 5.4d	• The maximum number of measurements is set to 509 (instead of 510) in the GOPR prototype.

17-MAR-2003	GOPR 5.4c	• Modification of the CAL ADFs (update of the limb radiometric LUT). The products are affected only if the limb spectra are converted into physical units • Modifications to allow compatibility with ACRI computational cluster (no modifications of the results) • Modification of the logic to handle dark charge map refresh at orbit level (DSA data is now directly processed by the level 1b processor if available in the level 0 product). No impact on the results
21-FEB-2003	GOPR 5.4b	• DC map values are rounded when written in the level 1b product • Modification of the CAL ADFs (update of the wavelength assignment of SPB1 and SPB2) • Modify the computation of flag_mod in the modulation correction routine
17-JAN-2003	GOPR 5.4a	• use the start and stop dates of the occultation when calling the CFI interpol instead of start and stop dates of the level 0 product • modify the ECMWF filename information in the SPH of the level 1b and limb products

5.1.2 AUXILIARY DATA FILES (ADF)

The ADF's files in tables 5.1-3, 5.1-4, 5.1-5, 5.1-6 and 5.1-7 have been disseminated to the PDS during the whole mission. For every type of file, the validity runs from the start validity time until the start validity time of the following one, but if an ADF file has been disseminated after the start validity time, it is obvious that it will be used by the PDHS-E and PDHS-K PDS only after the dissemination time (this happens the majority of the times). As the other ADF's, the calibration auxiliary file (GOM_CAL_AX) has been updated several times in the past (table 5.1-7) but the difference is that now it is updated in a weekly basis with only new DC maps, and that is why the files used in November are reported in a separate table (table 5.1-8) that will changed from month to month. On 2nd, 8th, 15th, 22nd and 29th November new calibration ADF's were disseminated with updated DC maps of orbits 13864, 13977, 14064, 14164, 14264 and 14365 respectively (table 5.1-8). Note that the files outlined in yellow are the set of auxiliary files used during the reporting period.

Table 5.1-3: Table of historic GOM_PR1_AX files used by PDS for level 1b products generation

Used by PDS for Level 1b products generation in period	GOM_PR1_AX (GOMOS processing level 1b configuration file)
01-MAR-2002 → 29-MAR-2002	**GOM_PR1_AXVIEC20020121_165314_20020101_000000_20200101_000000** • Pre-launch configuration
30-MAR-2002 → 14-NOV-2002	**GOM_PR1_AXVIEC20020329_115921_20020324_200000_20100101_000000** • Changed num_grid_upper, thr_conv and max_iter in the atmospheric GADS
Not used	**GOM_PR1_AXVIEC20020729_083756_20020301_000000_20100101_000000** • Cosmic Ray mode + threshold • DC correction based on maps • Non-linearity correction disabled
Not used	**GOM_PR1_AXVIEC20021112_170331_20020301_000000_20100101_000000** • Central background estimation by linear interpolation + associated thresholds

15-NOV-2002 → 26-MAR-2003	**GOM_PR1_AXVIEC20021114_153119_20020324_000000_20100101_000000** • Same content as GOM_PR1_AXVIEC20021112_170331_20020301_000000_20100101_000000 but validity start updated so as to supersede according to the PDS file selection rules GOM_PR1_AXVIEC20020329_115921_20020324_200000_20100101_000000
27-MAR-2003 → 19-MAR-2004	**GOM_PR1_AXVIEC20030326_085805_20020324_200000_20100101_000000** • Same content as GOM_PR1_AXVIEC20021112_170331_20020301_000000_20100101_000000 but validity start updated so as to supersede according to the PDS file selection rules GOM_PR1_AXVIEC20020329_115921_20020324_200000_20100101_000000
20-MAR-2004 → 22-MAR-2004	**GOM_PR1_AXVIEC20040319_134932_20020324_200000_20100101_000000** • Ray tracing parameter changed: convergence criteria set to 0.1 microrad
23-MAR-2004 → 01-APR-2004 *Notes*: • This file was constructed from GOM_PR1_AXVIEC20030326_085805_20020324_200000_20100101_000000 (so without the ray tracing parameter changed) • This file was used by the GOMOS/4.02 processors before the IECF dissemination. The dissemination was done on 25th March 2004	**GOM_PR1_AXVIEC20040316_144850_20020324_200000_20100101_000000** GOM_PR1 ADF for version GOMOS/4.02, changes: • The central band estimation mode • Atmosphere thickness • Altitude discretisation
02-APR-2004	**GOM_PR1_AXVIEC20040401_083133_20020324_200000_20100101_000000** • Ray tracing parameter changed: convergence criteria set to 0.1 microrad

Table 5.1-4: Table of historic GOM_INS_AX files used by PDS for level 1b products generation

Used by PDS for Level 1b products generation in period	GOM_INS_AX (GOMOS instrument characteristics file)
01-MAR-2002 → 29-JUL-2002	**GOM_INS_AXVIEC20020121_165107_20020101_000000_20200101_000000** • Pre-launch configuration
30-JUL-2002 → 12-NOV-2002	**GOM_INS_AXVIEC20020729_083625_20020301_000000_20100101_000000** • Factors for the conversion of the SFA angles from SFM axes to GOMOS axes
13-NOV-2002 → 16-JUL-2003	**GOM_INS_AXVIEC20021112_170146_20020301_000000_20100101_000000** • No more invalid spectral range
Not used	**GOM_INS_AXVIEC20030716_080112_20030711_120000_20100101_000000** • New value for SFM elevation zero offset for redundant chain: 10004
17-JUL-2003	**GOM_INS_AXVIEC20030716_105425_20030716_120000_20100101_000000** • Bias induct azimuth redundant value set to -0.0084 rad (-0.4813 deg)

Table 5.1-5: Table of historic GOM_CAT_AX files used by PDS for level 1b products generation

Used by PDS for Level 1b products generation in period	GOM_CAT_AX (GOMOS Stat Catalogue file)
01-MAR-2002	**GOM_CAT_AXVIEC20020121_161009_20020101_000000_20200101_000000** • Pre-launch configuration

Table 5.1-6: Table of historic GOM_STS_AX files used by PDS for level 1b products generation

Used by PDS for Level 1b products generation in period	GOM_STS_AX (GOMOS Star Spectra file)
01-MAR-2002	**GOM_STS_AXVIEC20020121_165822_20020101_000000_20200101_000000** • Pre-launch configuration

Table 5.1-7: Table of historic GOM_CAL_AX files used by PDS for level 1b products generation

Used by PDS for Level 1b products generation in period	GOM_CAL_AX (GOMOS Calibration file)
01-MAR-2002 → 29-JUL-2002	**GOM_CAL_AXVIEC20020121_164808_20020101_000000_20200101_000000** • Pre-launch configuration
Not used	**GOM_CAL_AXVIEC20020121_142519_20020101_000000_20200101_000000** • Pre-launch configuration
30-JUL-2002 → 12-NOV-2002	**GOM_CAL_AXVIEC20020729_082426_20020717_193500_20100101_000000** • Band setting information • Wavelength assignment • Spectral dispersion LUT • ADC offset for Spectrometers • PRNU maps • Thermistor coding LUT • DC maps
Not used	**GOM_CAL_AXVIEC20021112_165603_20020914_000000_20100101_000000** • Band setting information • DC maps • PRNU maps • Wavelength assignment • Spectral dispersion LUT • Radiometric sensitivity LUT (star and limb) • SP-FP intercalibration LUT • Vignetting LUT • Reflectivity LUT • ADC offset
13-NOV-2002 → 30-JAN-2003	**GOM_CAL_AXVIEC20021112_165948_20021019_000000_20100101_000000** • Only DC maps updated
31-JAN-2003 → 11-APR-2003	**GOM_CAL_AXVIEC20030130_133032_20030101_000000_20100101_000000** • Only DC maps updated (using DSA of orbit 04541)

12-APR-2003 → 02-JUN-2003	**GOM_CAL_AXVIEC20030411_065739_20030407_000000_20100101_000000** • Modification of the radiometric sensitivity curve for the limb spectra. Note that the modification of this LUT has no impact on the GOMOS processing. The LUT is just copied into the level 1b limb product for user conversion purpose. • Updated DC map only (using DSA of orbit 05762).
03-JUN-2003: from this date onwards, mainly updates to DC maps are done. Every month, the table of new GOM_CAL files with **only** DC maps updated is provided (table 5.1-8). Eventual changes to this file not corresponding only to DC maps updates will be reported in this table.	**GOM_CAL_AXVIEC20030602_094748_20030531_000000_20100101_000000** • Updated DC maps only (using DSA of orbit 06530)
13-FEB-2004 → 23-FEB-2004	**GOM_CAL_AXVIEC20040212_103916_20040209_000000_20100101_000000** • Update of the reflectivity LUT • Updated DC maps (Orbit 10194, date 11-FEB-2004)

Table 5.1-8: Calibration ADF for reporting period. These files are updated (only with DC maps) in a 7-10 days basis

Used by PDS for Level 1b products generation in period	GOM_CAL_AX (GOMOS Calibration file)
26-OCT-2004 → 02-NOV-2004	**GOM_CAL_AXVIEC20041025_144050_20041023_000000_20100101_000000** (orbit 13864, date 24-OCT-2004)
03-NOV-2004 →08-NOV-2004	**GOM_CAL_AXVIEC20041102_140742_20041031_000000_20100101_000000** (orbit 13977, date 01-NOV-2004)
09-NOV-2004 → 15-NOV-2004	**GOM_CAL_AXVIEC20041108_084144_20041106_000000_20100101_000000** (orbit 14064, date 07-NOV-2004)
16-NOV-2004 → 22-NOV-2004	**GOM_CAL_AXVIEC20041115_100546_20041113_000000_20100101_000000** (orbit 14164, date 14-NOV-2004)
23-NOV-2004 → 29-NOV-2004	**GOM_CAL_AXVIEC20041122_101637_20041120_000000_20100101_000000** (orbit 14264, date 20-NOV-2004)
30-NOV-2004 → 06-DEC-2004	**GOM_CAL_AXVIEC20041129_135000_20041127_000000_20100101_000000** (orbit 14365, date 28-NOV-2004)

5.2 Quality Flags Monitoring

In this section it is monitored some Product Quality information stored in level 1b products that did not have a fatal error (MPH error flag not set). The products with fatal errors were around 0.9% of the products received during November for the quality monitoring.

On the one hand, for every product we have information of the **number of measurements** where a given problem was detected (i.e. number of invalid measurements, number of measurements containing saturated samples, number of measurements with demodulation flag set…). On the other hand, there are **flags** that indicate problems within the product (i.e. flag set to one if the reference spectrum was computed from DB, flag set to zero if SATU data were not used…).

For the information on the number of measurements a plot of percentages with respect to time is provided in fig. 5.2-1. Part of this information, the most relevant one, is also plotted in a world map as a function

of ENVISAT position: % of cosmic ray hits per profile, % of datation errors per profile, % of star falling outside the central band per profile and % of saturation errors per profile (fig.5-2.2).

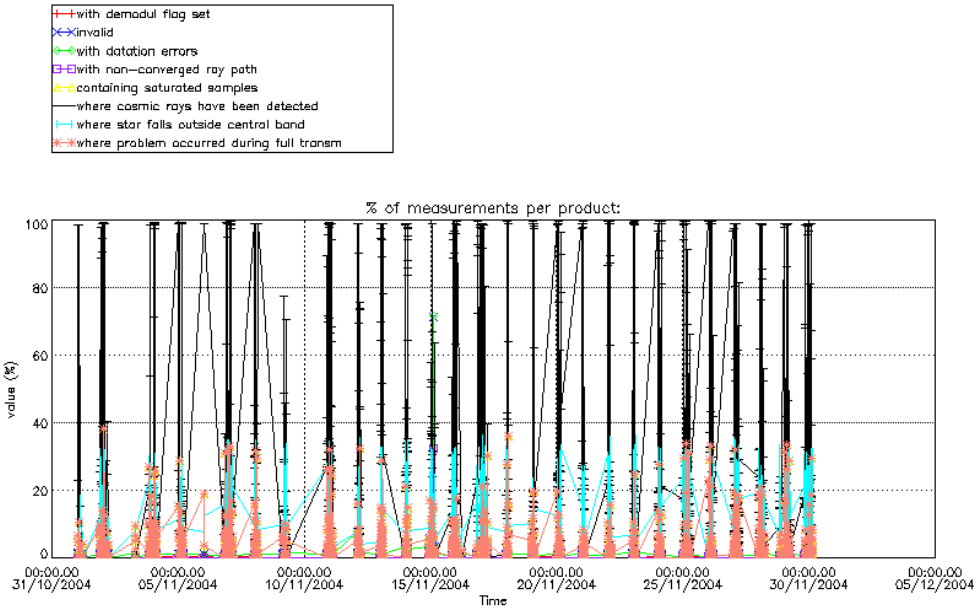

Figure 5.2-1: Level 1b product quality monitoring with respect to time

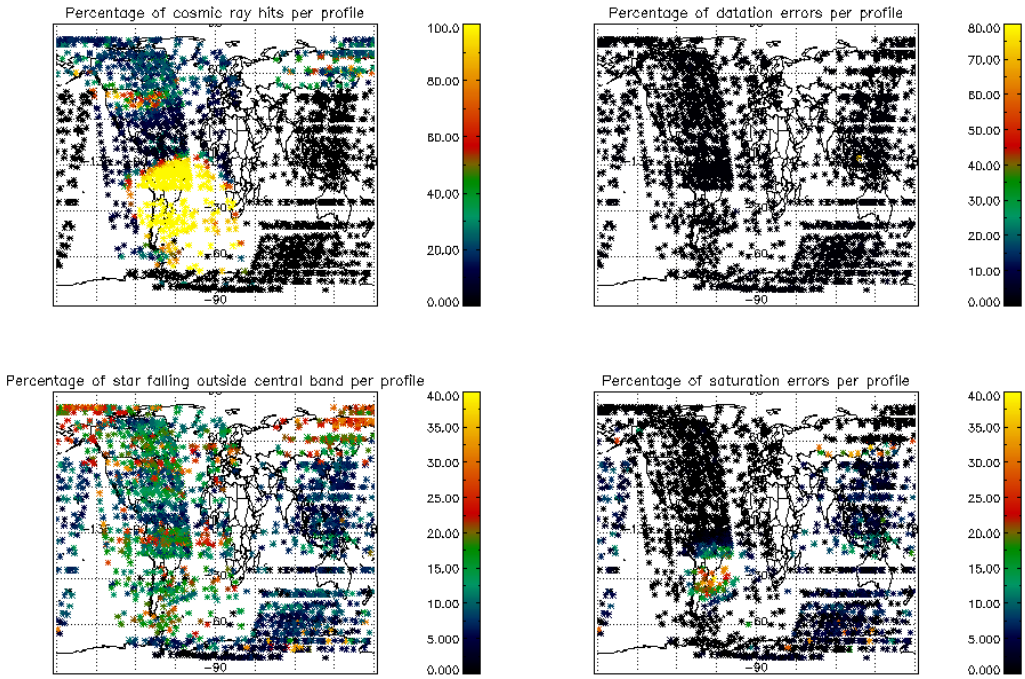

Figure 5.2-2: Level 1b product quality monitoring with respect to geo-location of ENVISAT

It can be seen from fig. 5.2-1 that the cosmic rays hits occurred several times for the 95% of the measurements of the products. Looking at fig. 5.2-2 it can be clearly observed that this high percentage occurred mainly when the satellite crossed the South Atlantic Anomaly (SAA) zone. High values are also observed over North America. Also the percentage of saturation errors per profile increased over SAA zone.
Another observation from fig. 5.2-1 is that, for many products, the 15-20 % of the measurements has the star signal falling outside the central band. In fig. 5.2-2 it is observed that this percentage occurred mainly during the ascending part of the orbit (night-side of the orbit) while in the descending part (day-side of the orbit) the percentage is less than 10 %. This is because during the night the stars are lost deeper within the atmosphere and the turbulence phenomena become more important, producing the star to be less 'focused' on the spectrometers central band. The other values (% of invalid measurements per product, % of measurements per product with datation errors…) are quite low.

The flag information is given in table 5.2-1. It is reported also the percentage of the products that have at least one measurement with demodulation flag set.

Table 5.2-1: Percentage of products during the reporting period with:

At least one measurement with demodulation flag set:	18.3206 %
Reference spectrum computed from DB:	0.00000 %
Reference spectrum with small number of measurements:	0.00000 %
SATU data not used:	0.00000 %

5.2.1 QUALITY FLAGS MONITORING (EXTRACTED FROM LEVEL 2 PRODUCTS)

In this section it is plotted the Product Quality information coming from the level 1 processing but stored also in the level 2 products. Only products that did not have a fatal error (MPH error flag not set) are considered. The purpose of using the level 2 data is simply that the percentage of level 2 products arriving in PCF for the quality monitoring is much higher. For November, 92% of the archived products have been received. The plots are very similar to fig. 5.2-1 and 5.2-2 (demodulation flag information is not included) but separating ascending from descending passes. The ascending part of the orbit (above -70^{o} latitude) is in dark limb while the descending (below 58^{o} latitude) is in bright limb.

Fig. 5.2-3 and 5.2-4 present some quality information as a function of the time whereas in fig. 5.2-5 and 5.2-6 the plot is respect to the satellite position at the beginning of the occultations. In ascending (fig. 5.2-5) the SAA is perfectly localized by the high percentage of cosmic ray hits per product (upper left panel). It is not the same if we look fig. 5.2-6, because in descending the most of the occultations are in bright limb conditions and the cosmic rays detection processing is not activated.

Another clear difference between ascending and descending is that in ascending (fig. 5.2-3) the percentage of measurements "where a problem occurred during the full transmission" per product is around 2% while for the descending passes is around 10%. This is due to the saturation that occurs mainly in bright limb. In ascending the saturation occurs over the SAA zone but it is quite low elsewhere.

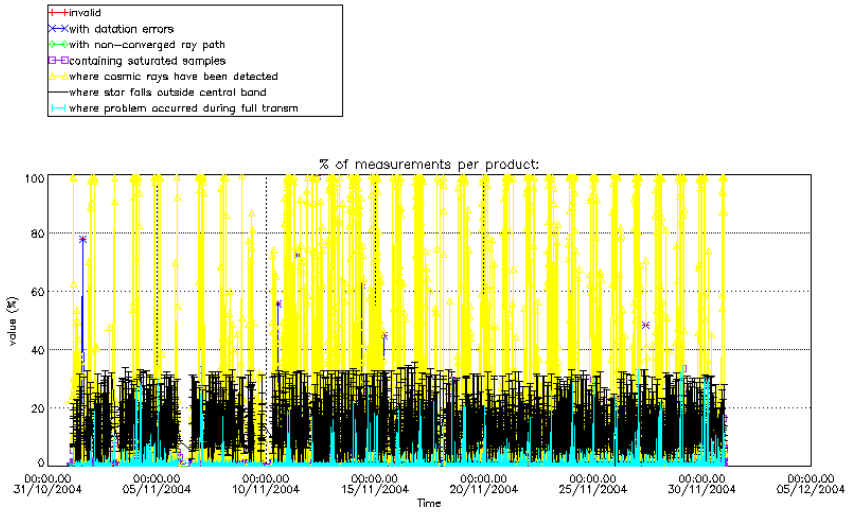

Figure 5.2-3: Level 1b product quality monitoring with respect to time ASCENDING ENVISAT passes

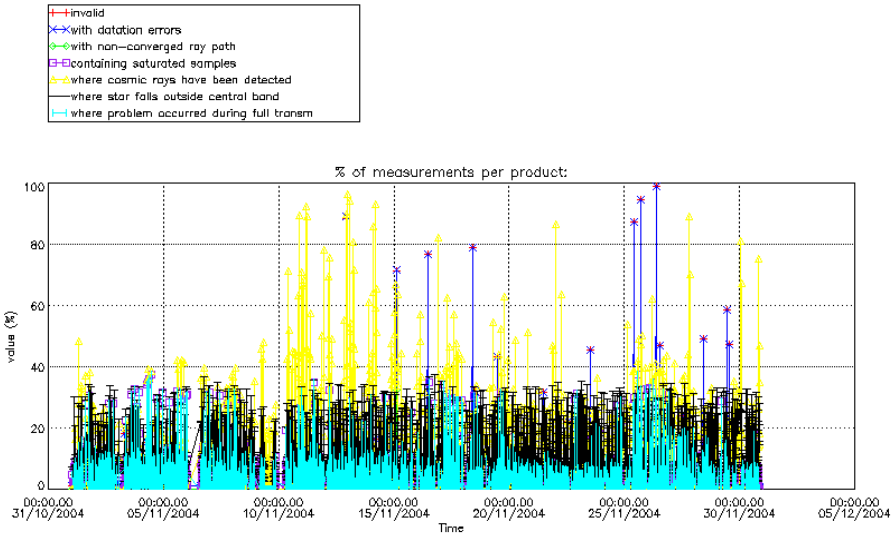

Figure 5.2-4: Level 1b product quality monitoring with respect to time DESCENDING ENVISAT passes

There are some products with a high percentage of invalid measurements and measurements with datation errors. These products are mostly coming from level 0 files with some acquisition failures that are occurring since November 2004. These products have a degraded quality and should not be used by the users.

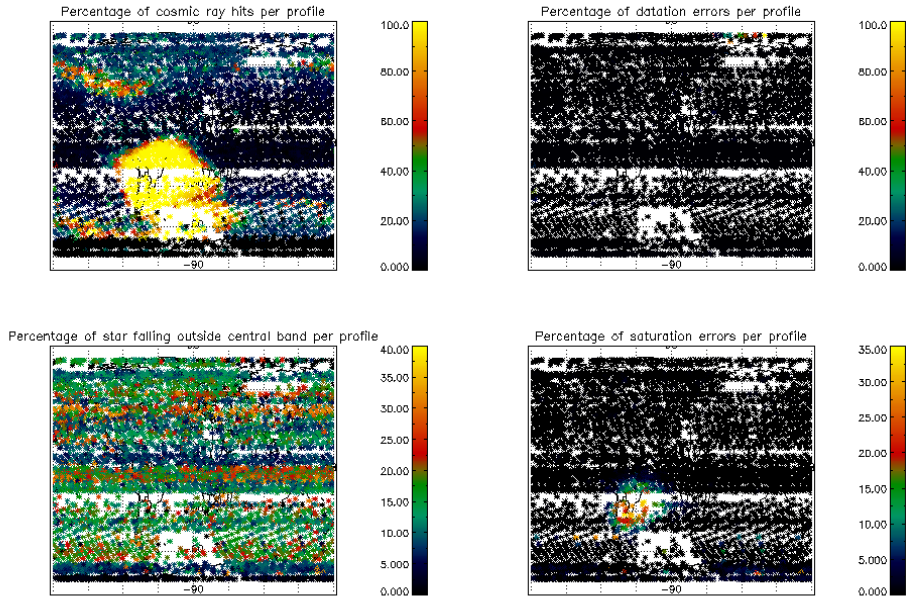

Figure 5.2-5: Level 1b product quality monitoring with respect to geolocation for <u>ASCENDING</u> ENVISAT passes

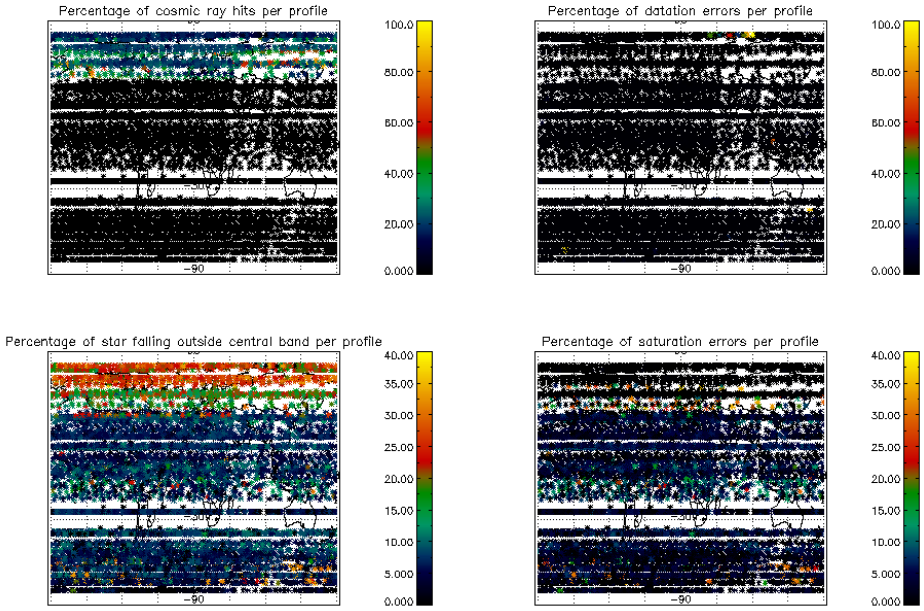

Figure 5.2-6: Level 1b product quality monitoring with respect to geolocation for <u>DESCENDING</u> ENVISAT passes

5.3 Spectral Performance

No new spectral calibration has been performed during the reporting period. Last calibration exercises have shown that warning values have been reached.

The values reported (table 5.3-1) are, for every star ID (1, 2, 4, 9, 18, 25), the wavelength of the first useful pixel of SPA2. This value is calculated by addition to the actual wavelength assignment, the spectral shift for which a maximum correlation has been found between the reference spectrum and the one of the occultation.

During the last wavelength calibration analysis performed using several occultations, the spectral shifts were 0.08 for star id number 1, 0.088 for star id number 2 and 0.095 for star ids number 9 & 18 (see table 5.3-1). These shifts are greater than 0.07 (warning value) and QWG investigations that have been initiated already in March will continue.

The star number 4 is left in table 5.3-1 even if the values of the wavelength are very different from the nominal one. It should be just kept in mind that the values of the shift should be always of the same order (~0.4) but this star will not be used for calibration purposes.

Table 5.3-1: Wavelength assignment calculated for several occultations since November 2002

Star ID / Level 0 date	1	2	4	9	18	25
20021112_062935	Occ.30: 690.455750	Occ.26: 690.458740		Occ.28: 690.492981		
20021219_102754		Occ.33: 690.468140	Occ.26: 690.875122			
20030101_151630	Occ.3: 690.445068	Occ.37: 690.466003	Occ.30: 690.878540			
20030110_121504		Occ.32: 690.465088	Occ.25: 690.882385			
20030201_090221						Occ.21: 690.492981
20030415_123156			Occ.29: 690.959534		Occ.20: 690.552002	Occ.28: 690.492981
20030419_170041			Occ.29: 690.957520		Occ.23: 690.555420	
20030428_072600					Occ.19: 690.553645	Occ.28: 690. 492981
20030717_053233				Occ. 22: 690.473816	Occ. 26: 690.446594	
20040123_091615	Occ.1: 690.400513 Occ.40: 690.401550	Occ.35: 690.415161	Occ.27: 690.852478			
20040222_065917			Occ.25: 690. 850830			Occ.21: 690. 492981
20040128_163559	Occ.3: 690.399414					Occ.23: 690. 492981
20040804_123934	Occ.20 690.411377	Occ.24 690.404724		Occ.25 690.397522	Occ.29 690.397156	

5.4 Radiometric Performance

5.4.1 RADIOMETRIC SENSITIVITY

The monitoring performed consists in the calculation of the radiometric sensitivity of each CCD by computing the ratio between parts of the reference spectrum using specific stars. The parts of spectrum used are:

- UV: 250–300 nm
- Yellow: 500–550 nm
- Red: 640–690 nm
- Ir1: 761-770 nm
- Ir2: 935-944 nm

For the spectrometers the ratios are with respect to the 'yellow' spectral range. For the photometers, the ratio is calculated dividing the mean photometer signal above the atmosphere (115 km) by the 'yellow' spectral range (for PH1) or by the 'red' spectral range (for PH2).

The variation of the ratio in percentage should be within a given threshold actually set to 10% (see table 5.4-1 that corresponds to fig. 5.4-1). For every star, this variation is calculated as the difference between the maximum (or minimum) ratio, and the mean over the 15 first values (if there are not 15 values computed yet, all values are used).

Table 5.4-1: Variation of RS for the different ratios (corresponds to fig. 5.4-1). Should be less than 10%

Star Id	% Variation of UV ratio	% Variation of Red ratio	% Variation of IR1 ratio	% Variation of IR2 ratio	% Variation of Ph1 ratio	% Variation of Ph2 ratio
1	2.04276	0.511867	0.401701	0.217333	30.8640	70.2278
2	0.416756	0.647292	0.625175	0.216532	4.52068	7.93166
4	0.106818	0.678080	1.17073	1.16053	8.08780	23.5227
9	4.63446	0.416139	0.783493	0.466555	835.855	2624.41
18	0.990748	0.681692	0.844914	0.852089	1865.10	5139.44
25	10.6943	0.699922	0.654513	1.12662	28.0870	147.396

Values outside the warning threshold set to 10% are observed mainly for the photometers, and investigations were performed by the QWG. An inaccurate reflectivity correction LUT was suspected to be the cause of the increase but a new one is in use since 12th February 2004 and the results did not change.

In fig. 5.4-2 the two fast photometer ratios have been splinted by stars, so one plot per star is presented. As it can be seen, for star id 9 only two points are the cause of the big variation of the percentage while for star id 18 it is just one point. This means that there is not a real problem in the radiometric sensitivity for the photometers even if the outliers exist and an explanation should be found. For star id 25, the problem is different. It is observed a real variation of the ratios but as it is only seen for this star, it can be concluded that the variation should be linked to the star itself and not to the photometers.

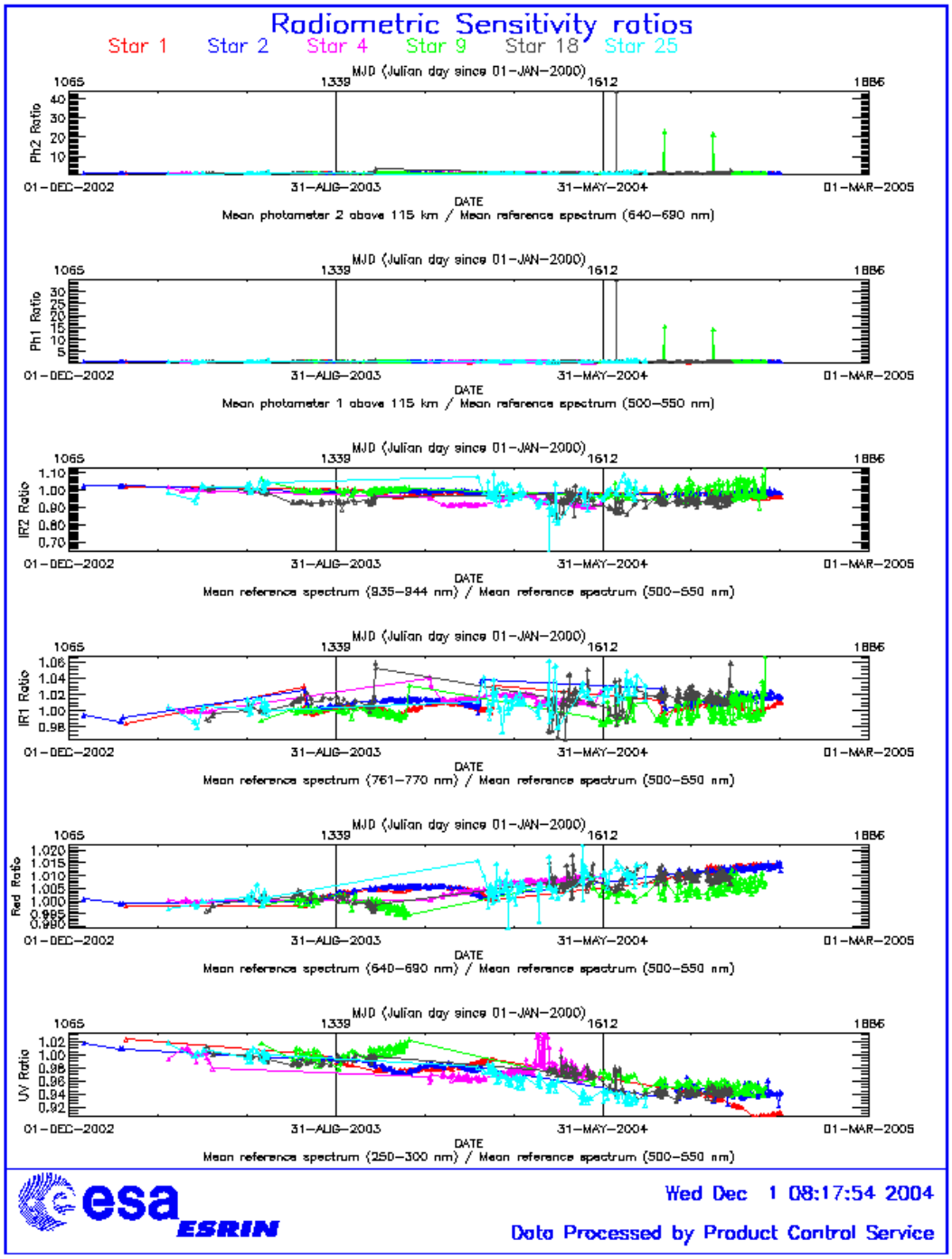

Figure 5.4-1: Radiometric sensitivity ratios since December 2002

For star 25 also the UV ratio is greater than 10%. Looking at the fig. 5.4-1, it is clear that there is a global decrease of UV ratios for all the stars. This confirms the expected degradation suffered by the UV optics that is, anyway, very small considering also the small variation for the rest of the stars (table 5.4-1).

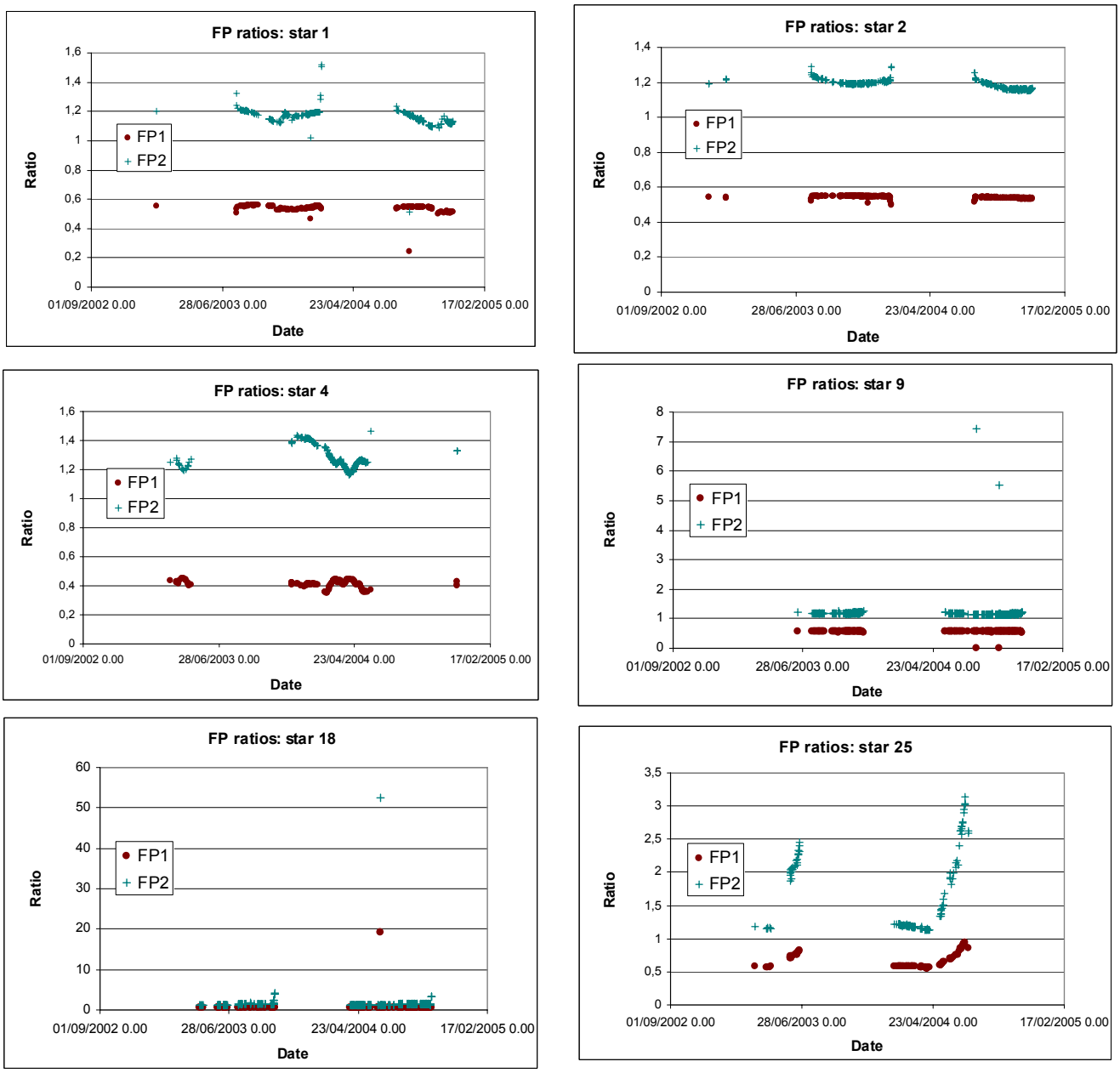

Figure 5.4-2: Fast Photometer ratios for the different monitoring stars. They are the same ratios plotted in fig. 5.4-1 (the ones corresponding to PH1 and PH2) but now one plot per star.

5.4.2 PIXEL RESPONSE NON UNIFORMITY

No new PRNU calibration has been performed during the reporting period. This means that the PRNU maps inside the ADF remain as they are without any change for the moment.

5.5 Other Calibration Results

Future reports will address other calibration results, when available.

6 LEVEL 2 PRODUCT QUALITY MONITORING

6.1 Processor Configuration

6.1.1 VERSION

Level 2 products from the operational ground segment have been disseminated during November to the users. About 92% of GOM_NL__2P products have been received in the PCF for routine quality control and long term trend monitoring. The current level 2-processor software version for the operational ground segment is GOMOS/4.02 (see table 6.1-1). The product specification is PO-RS-MDA-GS2009_10_3H. The improvements defined at the first Validation Workshop have been implemented into the prototype processor GOPR 6.0a (see table 6.1-2), before implementation into the operational one. In the mean time, Cal/Val teams are supplied with selected data sets generated by this prototype processor (version also used for the GOMOS reprocessing (see section 6.1.3)).

Table 6.1-1: PDS level 2 product version and main modifications implemented

Date	Version	Description of changes
23-MAR-2003	Level 2 version 4.02 at PDHS-E and PDHS-K	Algorithm baseline level 2 DPM 5.5: Section 3 • Add references to technical notes on Tikhonov regularization • Change High level breakdown of modules: SMO/PFG • Change parameter: NFS in l2 ADF • Change parameter σ_G in l2 ADF (Table 3.4.1.1-II) • Change content of Level 2/res products - GAP • Change time sampling discretisation • Add covariance matrix explanation Section 5 • Replace SMO by PFG VER-1/2: Depending on NFS, Apply either a Gaussian filter or a Tikhonov regularization to the vertical inversion matrix • Unit conversion applied on kernel matrix • Suppress VER-3 Section 6 • GOMOS Atmospheric Profile (GAP): not used in this version • Time sampling in equation (6.5.3.7-73)

		• See ref. [3] for more details
31-MAY-2003	Level 2 version 4.00 at PDHS-E and PDHS-K	Algorithm baseline level 2 DPM 5.4: • Revision of some default values • Add a new parameter • Transmission model computation: suppress tests on valid pixels and species • Apply a Gaussian filter to the vertical inversion matrix • Very low signal values are substituted by threshold value • See ref. [3] for more details
21-NOV-2002	Level 2 version 3.61 at PDHS-E and PDHS-K	Algorithm baseline level 2 DPM 5.3a: • Revision of some default values • Wording of test T11 • Dilution term computation of jend • Covariance computation scaling applied before and after • See ref. [3] for more details

Table 6.1-2: GOPR level 2 product version and main modifications implemented

Date	Version	Description of changes
17-MAR-2004	GOPR 6.0a	• Rename Turbulence MDS into High Resolution Temperature MDS (HRTP) • Add vertical resolution per species in local densities MDS • Add Solar zenith angle at tangent point and at satellite level in geolocation ADS • Add "tangent point density from external model" in geolocation ADS • Suppress contribution of "tangent point density from external model" in "local air density from GOMOS atmospheric profile" in geolocation ADS (to be completed)
18-AUG-2003	GOPR 5.4d	• Tikhonov regularisation is implemented
18-MAR-2003	GOPR 5.4b	• Modification to implement the computation of Tmodel for spectrometer B (in version 5.4b, the Tmodel for SPB is still set to 1)
30-JAN-2003	GOPR 5.4a	• Modifications for ACRI internal use only. No impact on level 2 products.

6.1.2 AUXILIARY DATA FILES (ADF)

The ADF's files in table 6.1-3 and 6.1-4 are used by the PDS to process the data from level 1 to level 2. For every type of file, the validity runs from the start validity time until the start validity time of the following one, but if an ADF file has been disseminated after the start validity time, it is obvious that it will be used by the PDHS-E and PDHS-K PDS only after the dissemination time (this happens the majority of the times).

Table 6.1-3: Table of historic GOM_PR2_AX files used by PDS for level 2 products generation

Used by PDS for Level 2 products generation in period	GOM_PR2_AX (GOMOS Processing level 2 configuration file)
01-MAR-2002 → 29-JUL-2002	**GOM_PR2_AXVIEC20020121_165624_20020101_000000_20200101_000000** • Pre-launch configuration
30-JUL-2002 → 02-SEP-2002	**GOM_PR2_AXVIEC20020729_083851_20020301_000000_20100101_000000** • Maximum value of chi2 before a warning flag is raised (set to 5) • Maximum number of iterations for the main loop (set to 1)
03-SEP-2002 → 12-NOV-2003	**GOM_PR2_AXVIEC20020902_151029_20020301_000000_20100101_000000** • Maximum value of chi2 before a warning flag is raised (set to 100)
13-NOV-2003 → 22-MAR-2004	**GOM_PR2_AXVIEC20021112_170458_20020301_000000_20100101_000000** • Smoothing mode • Hanning filter • Number of iterations • Spectral windows to suppress the O2 absorption in the high spectral range of SPA2
23-MAR-2004 *Note*: this file was used by the GOMOS/4.02 processors before the IECF dissemination. The dissemination was done on 25th March 2004	**GOM_PR2_AXVIEC20040316_145613_20020301_000000_20100101_000000** • Pressure at the top of the atmosphere • Number of GOMOS sources data (used in GAP) • Activation flag for GOMOS sources data (GAP) • Smoothing mode (after the spectral inversion) • Atmosphere thickness

Table 6.1-4: Table of historic GOM_CRS_AX files used by PDS for level 2 products generation

Used by PDS for Level 2 products generation in period	GOM_CRS_AX (GOMOS Cross Sections file)
01-MAR-2002 → 08-MAR-2002	**GOM_CRS_AXVIEC20020121_164026_20020101_000000_20200101_000000** • Pre-launch configuration
09-MAR-2003 → 29-JUL-2002	**GOM_CRS_AXVIEC20020308_185417_20020101_000000_20200101_000000** • Corrected NUM_DSD in MPH - was 14 and is now 19 - and corrected spare DSD format by replacing last spare by carriage returns in file GOM_CRS_AXVIEC20020121_164026_20020101_000000_20200101_000000
30-JUL-2002 → 25-MAR-2004	**GOM_CRS_AXVIEC20020729_082931_20020301_000000_20100101_000000** • O3 cross-sections summary description (SPA) • NO3 cross-sections summary description • O2 transmissions summary description • H2O transmissions summary description • O3 cross sections (SPA)
26-MAR-2004 *Note*: the file was disseminated on 27 Jan 2004 but could not be used by PDS until version GOMOS/4.02 was in operation	**GOM_CRS_AXVIEC20040127_150241_20020301_000000_20100101_000000** • Update of the O2 and H2O transmissions (S.A input) • Extension by continuity of the O3 cross-section for SPB

6.1.3 RE-PROCESSING STATUS

For many reasons, not only PDS, but also the status of the Calibration and Validation activities at the end of the commissioning phase and the status of the processors (all these points being linked together), it has

been very difficult to distribute good products to the user community. To support the Calibration and Validation activities, some products have been generated using the prototypes and disseminated by the ESL on dedicated platforms. It is important to provide, not only to the Calibration and Validation teams but also to all the user community complete data sets for the period 2002 – 2003 of Level 1b and Level 2 products, reprocessed from a completed consolidated Level 0 data set. Data can be retrieved via web query from http://www.enviport.org/gomos/index.jsp. FTP access to bulk reprocessing results (one tar file of GOMOS products per day) is allowed from the D-PAC: ftp://gomo2usr@ftp-ops.de.envisat.esa.int.

The table 6.1-5 presents the status of the GOMOS reprocessing task in terms of availability of the instrument, level 0 input products and level 1b/2 output products. The status is presented by cycle. Each cycle is made of 501 orbits or 35 days. The last three columns of the table indicate the percentage of availability of each item with respect to the instrument availability in observation mode (i.e. for example without taking account the calibration or DSA observation of GOMOS).Values greater than 100% may occur due to the fact that some calibration observations are not taken into account in the instrument availability but they can be processed. See more details on http://www.fr-acri.com/gomval_web/news/board.htm

Table 6.1-5: Summary of reprocessing status at ACRI

Cycle	Orbits	Cycle Time Interval	% Instr. Availability	% L0 in ACRI	% Lv1b/L2 in ACRI
5	556-1056	08/04/02 21:59 - 13/05/02 20:18	89.6	0.0	0.0
6	1057-1557	13/05/02 21:59 -17/06/02 20:18	86.4	0.0	0.0
7	1558-2058	17/06/02 21:59 - 22/07/02 20:18	88.8	0.2	0.0
8	2059-2559	22/07/02 21:59 - 26/08/02 20:18	88.0	0.0	0.0
9	2560-3060	26/08/02 21:59 - 30/09/02 20:18	75.0	7.2	0.0
10	3061-3561	30/09/02 21:59 - 04/11/02 20:18	95.4	2.7	0.0
11	3562-4062	04/11/02 21:59 - 09/12/02 20:18	88.4	0.0	0.0
12	4063-4563	09/12/02 21:59 - 13/01/03 20:18	95.0	0.0	0.0
13	4564-5064	13/01/03 21:59 - 17/02/03 20:18	97.4	78.7	78.5
14	5065-5565	17/02/03 21:59 - 24/03/03 20:18	60.7	95.7	95.4
15	5566-6066	24/03/03 21:59 - 28/04/03 20:19	84.6	77.4	75.2
16	6067-6567	28/04/03 21:59 - 02/06/03 20:18	14.0	94.3	94.3
17	6568-7068	02/06/03 21:59 - 07/07/03 20:19	52.9	85.7	84.9
18	7069-7569	07/07/03 21:59 - 11/08/03 20:19	65.1	97.2	97.2
19	7570-8070	11/08/03 21:59 - 15/09/03 20:19	84.0	95.2	94.3
20	8071-8571	15/09/03 21:59 - 20/10/03 20:19	93.6	97.2	96.8
21	8572-9072	20/10/03 21:59 - 24/11/03 20:19	92.6	98.9	98.1
22	9073-9573	24/11/03 21:59 - 29/12/03 20:19	90.6	102.8	102.8
23	9574-10074	29/12/03 21:59 - 02/02/04 20:19	95.0	0.0	0.0
24	10075-10575	02/02/04 21:59 - 08/03/04 20:19	95.2	0.0	0.0
25	10576-11076	08/03/04 21:59 - 12/04/04 20:19	96.6	0.0	0.0
26	11077-11577	12/04/04 21:59 - 17/05/04 20:19	100.0	0.0	0.0
27	11578-12078	17/05/04 21:59 - 21/06/04 20:19	46.3	0.0	0.0
28	12079-12579	21/06/04 21:59 - 26/07/04 20:19	0.0	0.0	0.0
29	12580-13080	26/07/04 21:59 - 30/08/04 20:19	0.0	0.0	0.0

6.2 Quality Flags Monitoring

In this section it is plotted some information contained in the Quality Summary data set of the level 2 products of November. In particular, it is depicted the percentage of flagged points per profile for the local species O_3, H_2O, NO_2 and Air. Only products in dark limb illumination conditions and

without fatal errors (error flag in the MPH set to "0") are used. The products with fatal errors were around 0.5% of the products received during this month for the quality monitoring.

A profile point in a level 2 product is flagged when:

- The local density is less than a given minimum value
- The local density is greater than a given maximum value
- A negative local density was found
- The line density is not valid. And it occurs when:
    - The acquisition from level 1b is not valid
    - There is no acquisition used for reference star spectrum
    - The line density is less than a given minimum value
    - The line density is greater than a given maximum value
    - A negative line density was found

  For species: air, aerosol, O_3, NO_2, NO_3, OClO
    - No convergence after a given number of LMA iterations
    - χ^2 out of LMA is bigger than χ^2
    - Failure of inversion

  For species: O_2, H_2O
    - Spectro B only: no convergence
    - Spectro B only: data not available
    - Spectro B only: covariance not available

And the users should not use these flagged points for their applications.

Looking at the fig. 6.2-1 the most evident characteristic that can be observed is the high percentage of flagged points per profile for H_2O. Users should not use these data, as their quality is still poor. The percentage of flagged points per profile for O_3 and Air is around 35% whereas for NO_2 it becomes 60%. On 9th November from 09:44 to 18:07 all species have almost the whole profile points flagged. This is because for that period a special request was done in order to observe all stars outside the atmosphere with an altitude range between 310 and 100 km (note that the nominal one is from 130 to 5 km).

The same information is plotted in fig. 6.2-2 as a function of the first tangent point of every profile. There are points mainly between +60 and -52 degrees latitude because in this period of the year (autumn) full dark illumination condition occultations (only those products have been used for these plots) are found on that region. In summer, full dark illumination data are mainly in the Southern Hemisphere while in winter it is contrary: full dark illumination occultations will be found mainly in the Northern Hemisphere.

It can be seen that there are latitudinal bands with almost the same color (same percentages). This means that the percentages of flagged points per profile have a dependence on the stars that have been observed: a given star is always observed at the same latitude but at different longitude.

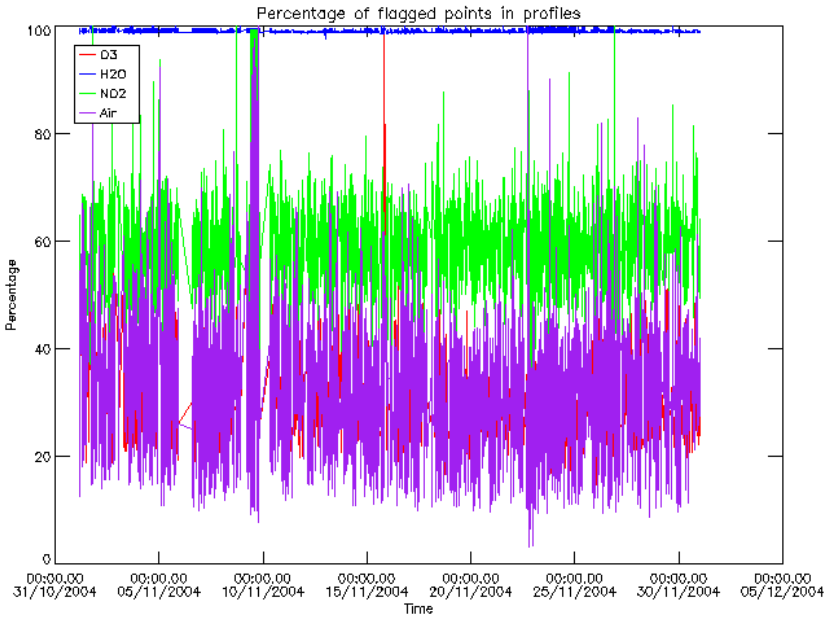

Figure 6.2-1: Percentage of flagged points per profile

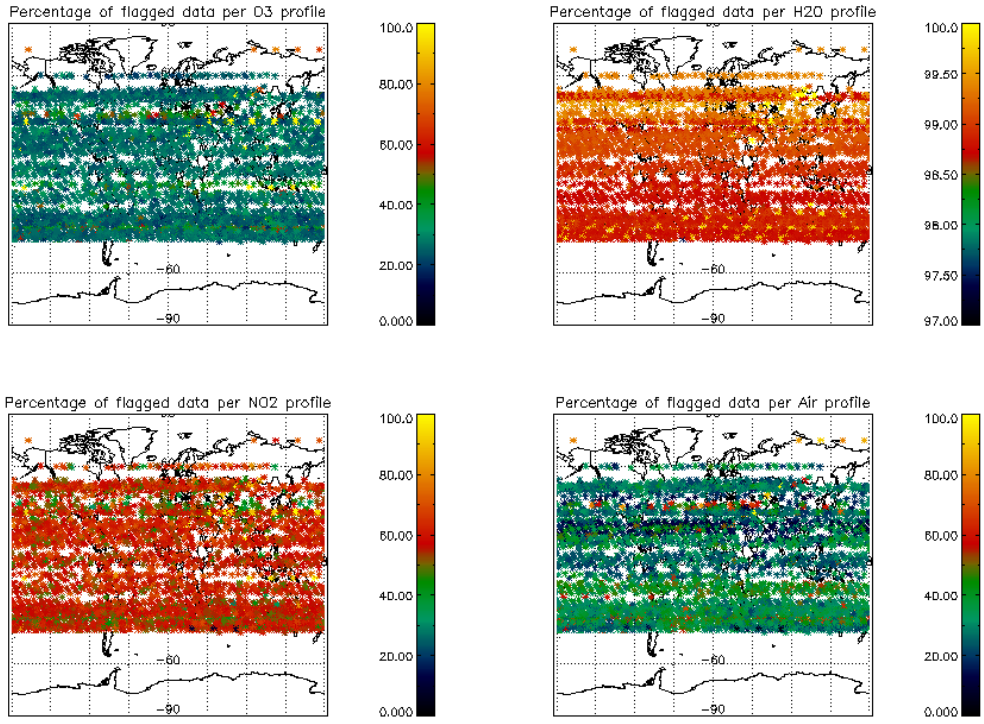

Figure 6.2-2: Percentage of flagged points per profile as a function of the first tangent point of the profile

6.3 Other Level 2 Performance Issues

6.3.1 MONTHLY AVERAGE OF O_3 PROFILES

The plot presented in fig. 6.3-1 is the average of the Ozone values during November in a grid of 0.5 degrees in latitude per 1 km in altitude. Only occultations in dark limb illumination conditions have been used. Some known characteristics can be seen:

- O_3 concentrations show a decrease with latitude near 40 km altitude. In the lower latitudes O_3 is generated by photolysis of O_2
- In the middle stratosphere (25-30 km) O_3 is strongly influenced by transport effects. Strong meridional and zonal transport is visible in middle and higher latitudes
- The lower stratosphere shows an O_3 increase with latitude. Highest values can be found within the polar regions due to downward transport of rich air masses

However, other characteristics seem not to be realistic as the values below 15 km, where data are not reliable at the moment or some high values at –45 degrees latitude at high altitude (suspected to be related to the SAA and currently under investigation).

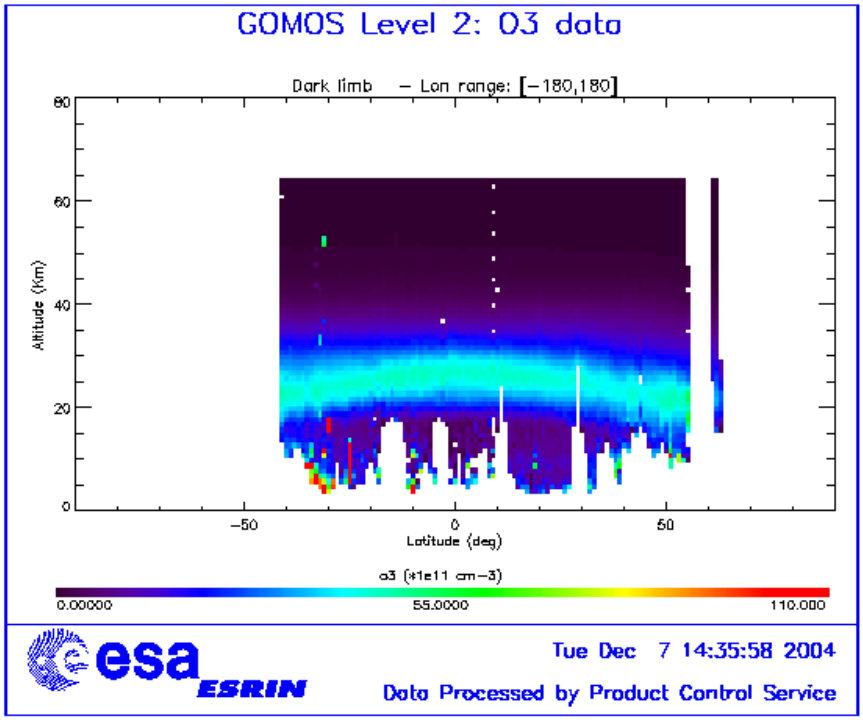

Figure 6.3-1: Average GOMOS O_3 profile during November: average in a grid of 0.5° latitude x 1 km altitude

6.3.2 DISTRIBUTION OF THE STANDARD DEVIATION OF O_2 OUTLIERS VALUES

It is presented here results on the assessment of GOMOS Level 2 products obtained during cycle number 22. We focus on the first 2000 vertical profiles measured in full dark mode (orbits between 9073 and 9292). Those data were reprocessed with GOPR version 6.0a (future IPF version 5.0). It is also presented the results of data reprocessed with a slightly modified version of GOPR. With this version, the contamination by O_2 emission in the spectrometer B is removed by using a background correction even in dark limb illumination condition. It is thus expected an improvement of the species which concentration is inferred from Spectrometer B, such as O_2, for data processed with this new version. Data processed with GOPR version 6.0a are referred as v6.0a6.0a data, and data processed with the modified version of GOPR are referred as 6.0b6.0a data.

Fig. 6.3-2 plots the histogram of the standard deviation of O_2 values, for the lowest 10% and the highest 10% O_2 values between 25km and 35km, for 2000 full dark measurements of cycle 22 (GOPR version 6.0a6.0a). The standard deviation of nearly half of the O_2 outliers is lower than 10%. For less than 10% of outliers, the standard deviation is between 10% and 20%, and this number is regularly decreasing until values of standard deviation higher than 100% (about 15% of the O_2 outliers).

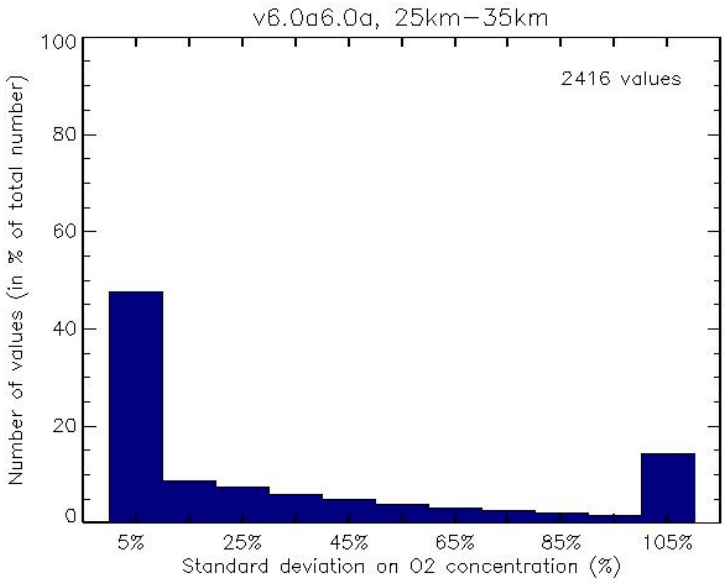

Figure 6.3-2: Histogram of the standard deviation of O_2 values (%), for O_2 concentration outliers (the lower 10% and the higher 10% of all O_2 concentration values) for 2000 full dark measurements of cycle 22 (GOPR version 6.0a6.0a), between 25km and 35km. Only non-flagged O_2 concentrations are considered. The number of values is given as the percentage of the total number of outliers. The last column actually includes all standard deviation values higher than 100%

When using GOMOS profiles processed with GOPR v6.0b6.0a (fig. 6.3-3), the standard deviation of more than 60% of the outliers is lower than 10%, the standard deviation of about 15% is between 10% and 20%, and the number of outliers with a standard deviation higher than 100% is lower than for version 6.0a6.0 (less than 10%).

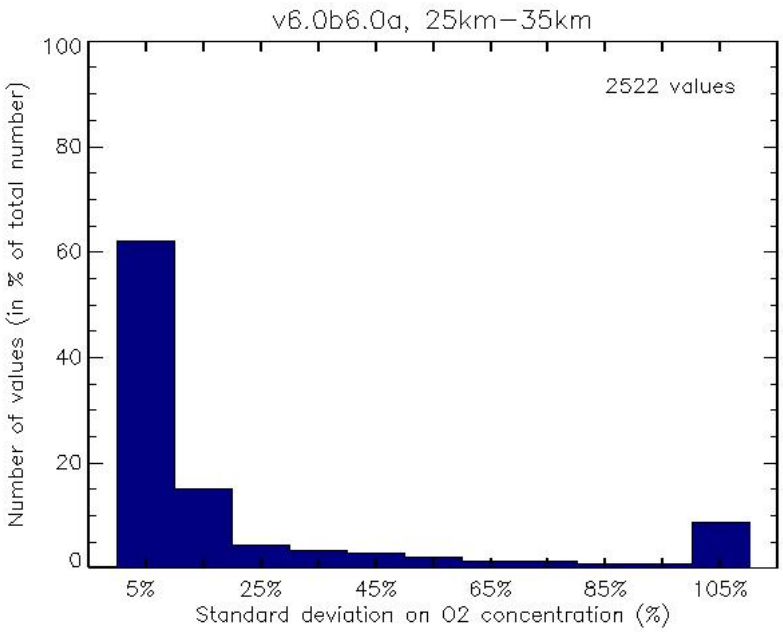

Figure 6.3-3: Same as fig. 6.3-2, for 2000 full dark measurements of cycle 22 (GOPR version 6.0b6.0a)

Fig. 6.3-4 plot the histograms of the standard deviation of the whole dataset of O_2 values (GOPR v6.0a6.0a and GOPR v6.0b6.0a respectively) between 25km and 35km. The distribution is not very different from the distribution of the standard deviation of the outliers, showing a large number of O_2 values with a standard deviation lower than 10%, and a significant number of O_2 values with a standard deviation higher than 100%.

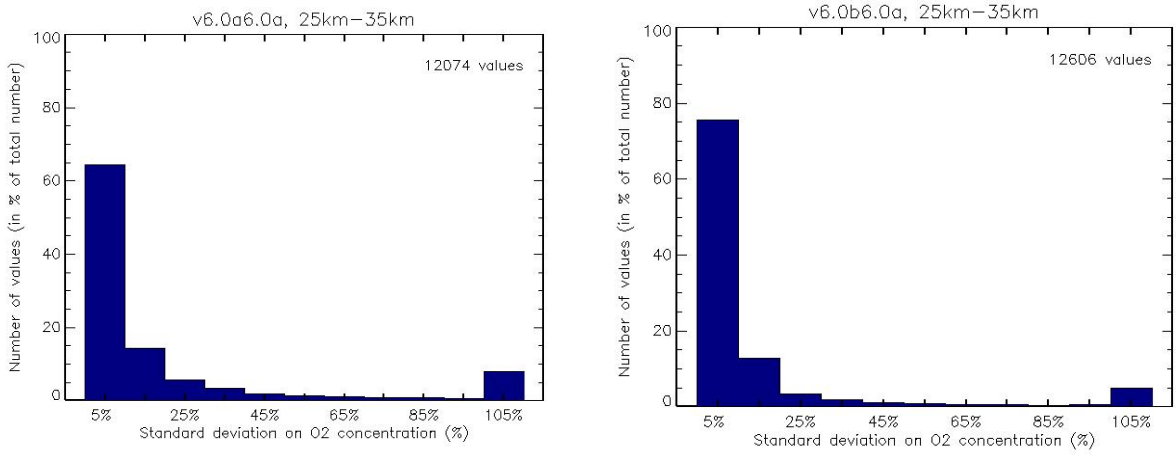

Figure 6.3-4: Same as fig. 6.3-2, but for the complete dataset of O_2 values between 25km and 35km. Left is using GOPR v6.0a6.0a, right is using GOPR v6.0b6.0a

It is concluded that the distribution of the standard deviation of the outlier values in O_2 concentration between 25km and 35km is very similar to the distribution of all the O_2 values in this altitude range.

6.3.3 DISTRIBUTION OF THE STANDARD DEVIATION OF CONCENTRATION VALUES FOR OTHER SPECIES

It is plotted here the distribution of the standard deviation for O_3, NO_2, NO_3 and H_2O concentration values within several altitude ranges, for 2000 full dark measurements of cycle 22 (GOPR version 6.0a6.0a).

For O_3 above 20km and H_2O below 20km, the distribution is quite similar at all altitude ranges: a large majority of values (about or above 70% of them) has a standard deviation lower than 10%. A small percentage (or none of them for O_3 between 20km and 40km) has a standard deviation higher than 20%.
For O_3 below 20km, as for NO_2 between 20km and 50km, and H_2O above 20km, the distribution is wider, with a lower relative number of values lower than 20%, and a significant relative number of standard deviation values higher than 100%.
For NO_2 below 20km, and for NO_3, the highest relative number of the distribution is for values of standard deviation higher than 100%. Only a small number of concentration values have standard deviation values lower than 20%.

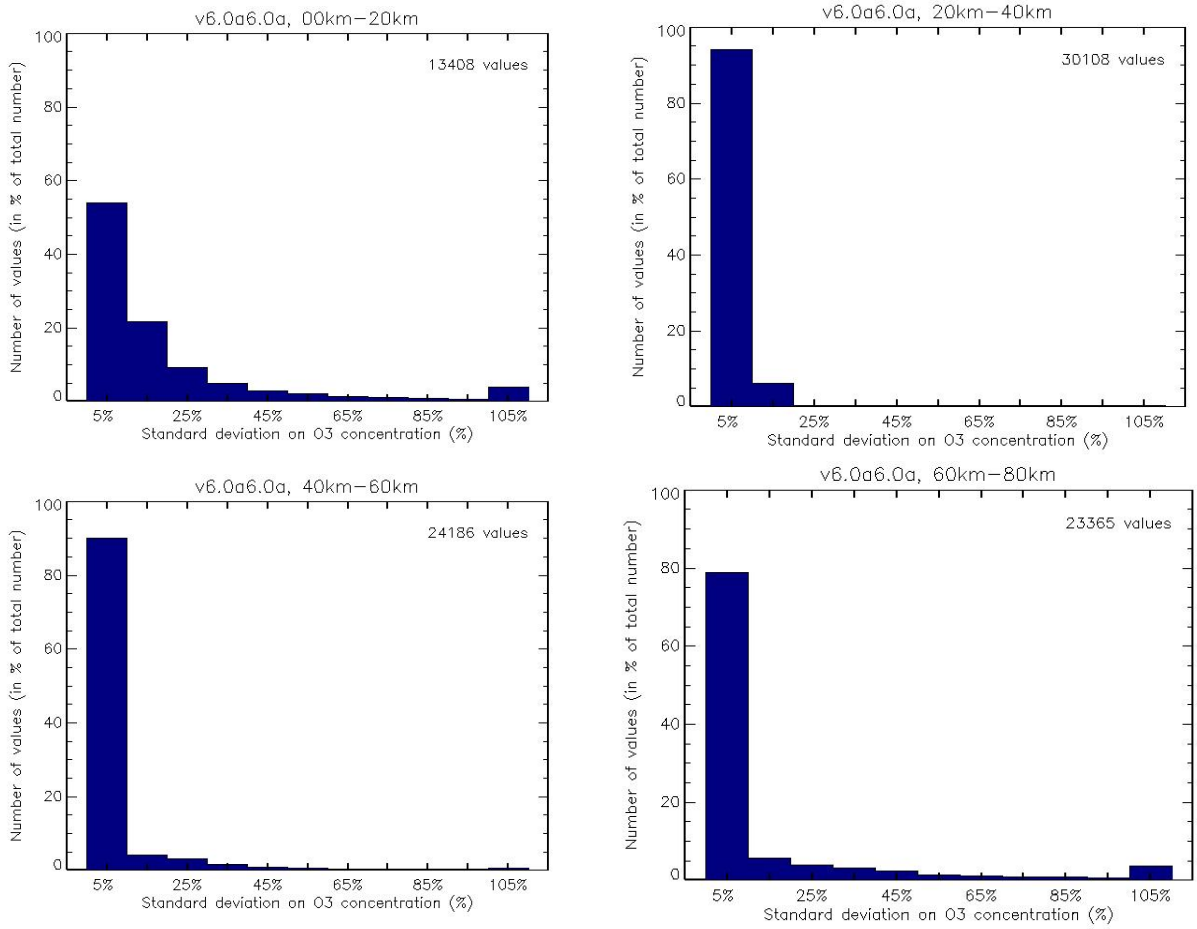

Figure 6.3-5: Histograms of the standard deviation of O_3 values (%), for 2000 full dark measurements of cycle 22 (GOPR version 6.0a6.0a), at different altitudes ranges. Only non-flagged O_3 concentrations are considered. The number of values is given as the percentage of the total number of values. The last column of the histograms actually includes all standard deviation values higher than 100%

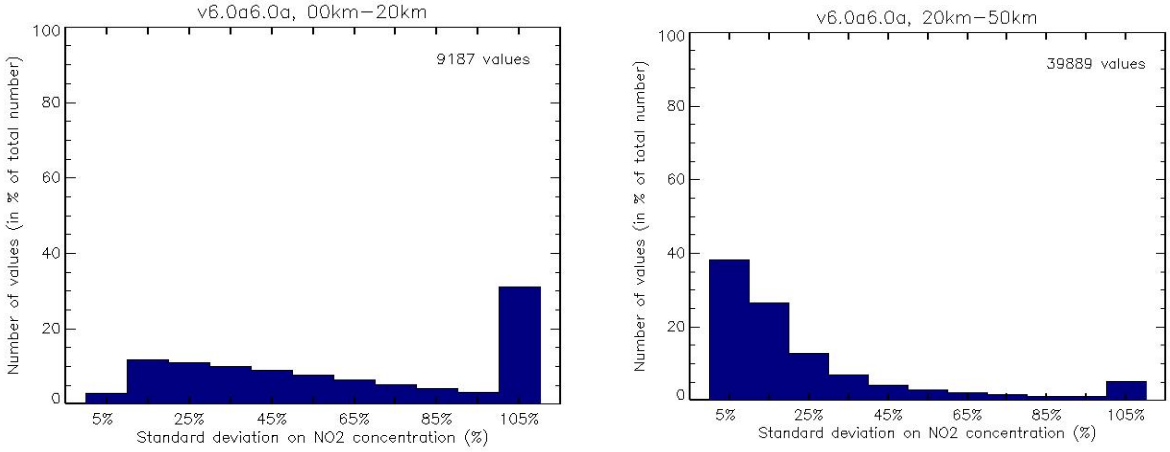

Figure 6.3-6: Same as fig 6.3-5, for the standard deviation of NO_2 concentration values at altitudes lower than 20km (left) and between 20-40 km (right)

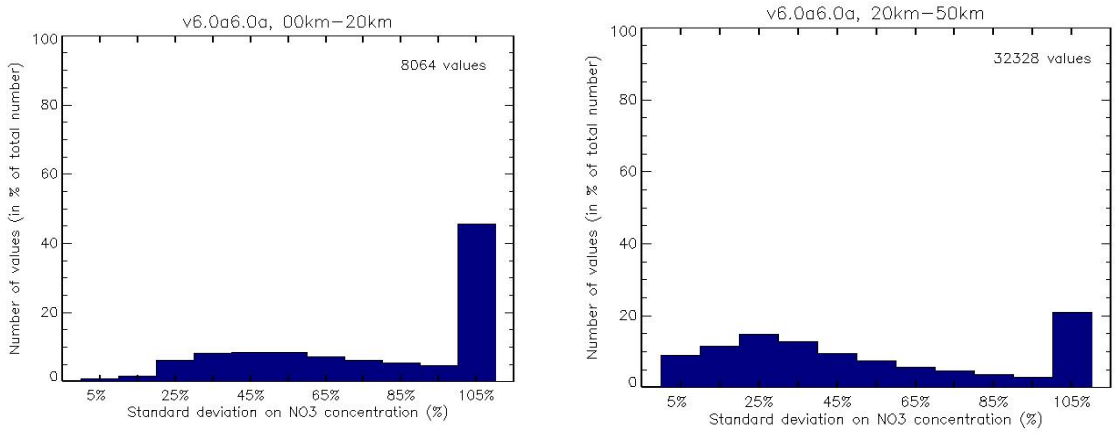

Figure 6.3-7: Same as fig. 6.3-5, for the standard deviation of NO_3 concentration values at altitudes lower than 20 km (left) and between 20-50 km

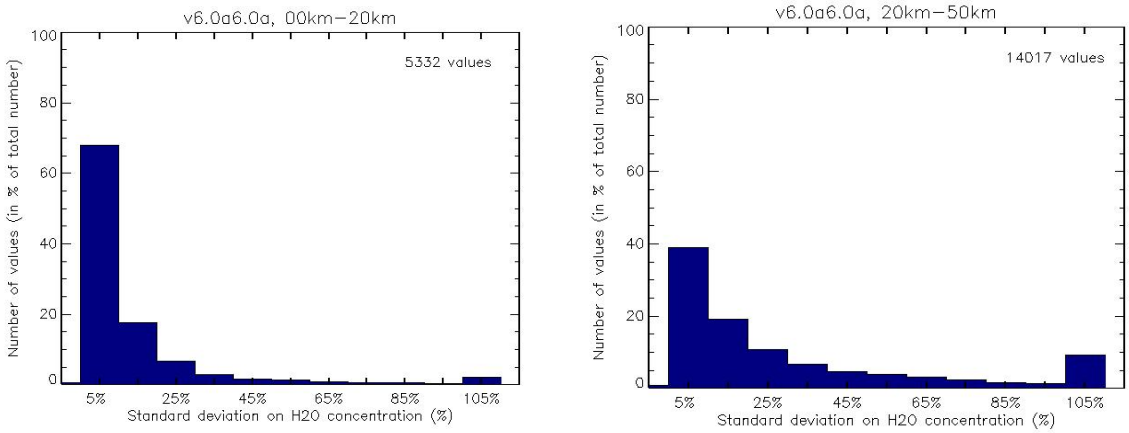

Figure 6.3-8: Same as fig. 6.3-5, for the standard deviation of H_2O concentration values at altitudes lower than 20 km (left) and between 20-50 km

7 VALIDATION ACTIVITIES AND RESULTS

7.1 GOMOS-ECMWF Comparisons

7.1.1 TEMPERATURE AND OZONE COMPARISONS

Due to restrictions in the current METEO product format, filtering of METEO data is not possible. ECMWF results are therefore partially based on data that are not to be used for scientific application, as mentioned in the disclaimer (http://envisat.esa.int/dataproducts/availability/disclaimers)

Summary of ECMWF GOMOS monthly report for November data (GOM_RR__2P):

- Overall good agreement between GOMOS and ECMWF temperatures.
- GOMOS temperatures are lower than ECMWF temperatures in most of the stratosphere and mesosphere, but area mean departures are less than 1% in most of the stratosphere. Larger departures are found at the model top.
- Large differences between GOMOS and ECMWF ozone values (over 50% in places).
- Large scatter of GOMOS ozone data.
- Scatter plots still show some unrealistically low GOMOS ozone values.
- No water vapour data in NRT GOMOS BUFR files.
- The monitoring statistics for November were produced with the operational ECMWF model, CY28R3.

The full November ECMWF report can be found in the links below:
http://earth.esa.int/pcs/envisat/gomos/reports/ecmwf_gomos_monthly_200411.pdf → text
http://earth.esa.int/pcs/envisat/gomos/reports/ecmwf_gomos_monthly_temp_200411.pdf → T plots
http://earth.esa.int/pcs/envisat/gomos/reports/ecmwf_gomos_monthly_o3_200411.pdf → O_3 plots

7.2 GOMOS-Climatology comparisons

Results will be presented upon availability.

7.3 GOMOS Assimilation

Results will be presented upon availability.

7.4 Consistency Verification: GOMOS-GOMOS Inter-comparison

7.4.1 H_2O COMPARISONS

Though H_2O profiles are also retrieved from measurements made with Spectrometer B, the contamination by O_2 emission affects less the spectral range used to retrieve H_2O concentrations than the spectral range

used to retrieve O_2 concentrations. Thus it is not expected the same improvement on H_2O concentrations as on O_2 concentrations when removing the contamination by O_2 emission in the spectrometer B.

Left panel of fig. 7.4-1 plots the values of H_2O concentration for 2000 full dark measurements of cycle 22 processed with GOPR v6.0a6.0a. In the upper troposphere/lower stratosphere, one can note the large values (up to and above 10^{15} mol.cm^{-3}), rapidly decreasing with the altitude down to or less than 10^{13} mol.cm^{-3}. Besides this global behaviour, many outliers make the profiles very noisy, especially above 20km. The same measurements processed with GOPR v6.0b6.0a are plotted on the right panel of fig. 7.4-1. As expected, there is no dramatic improvement of the H_2O quantities when processed with this modified version of the prototype. The only possible difference may be the slightly lower number of outliers (for instance around 20km).

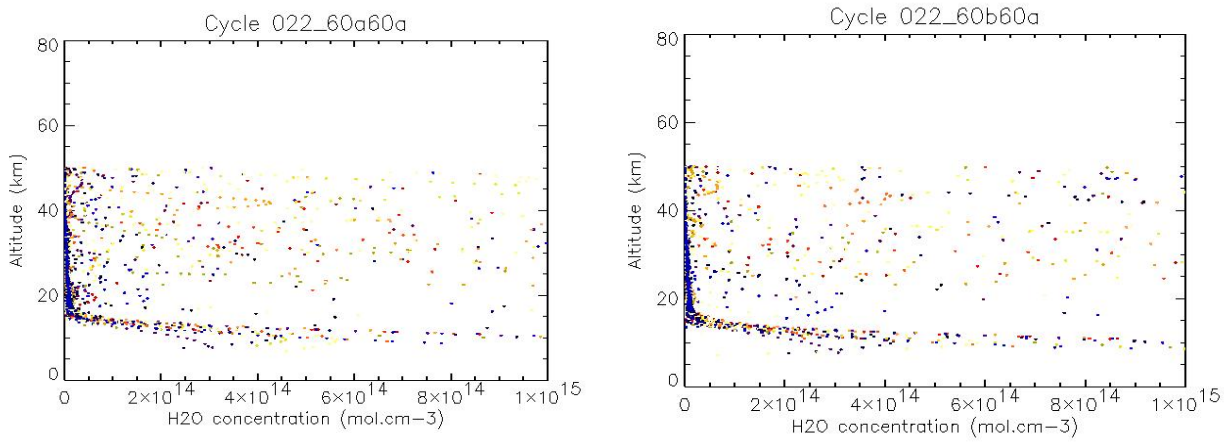

Figure 7.4-1: H_2O concentration versus altitude for 2000 full dark measurements of cycle 22. Individual profiles are plotted with different colours (but the same colour may be used to plot several profiles). GOPR version 6.0a6.0a is used for left panel, GOPR version 6.0b6.0a for right panel

At this early stage of the assessment of GOMOS H_2O values, it is plotted the H_2O results in concentration rather than in mixing ratio, because it is the quantity stored in the GOMOS Level2 products. As seen the large number of outliers on vertical profiles of concentration, the vertical profiles of mixing ratio would probably be even noisier.

The values of the difference between GOMOS H_2O concentration processed with GOPR v6.0b6.0a and GOMOS H_2O concentration processed with GOPR v6.0a6.0a are plotted versus altitude on fig. 7.4-2. Most of the difference values are cantered around 0 with a median difference lower than 10% up to 40km, but a large number of differences are much higher in amplitude. As for the comparison between O_2 by GOMOS and O_2 by ECMWF, there is a strong effect of the star magnitude, *i.e.* the amplitude of the difference between the two datasets is lower for measurements inferred from brighter stars.

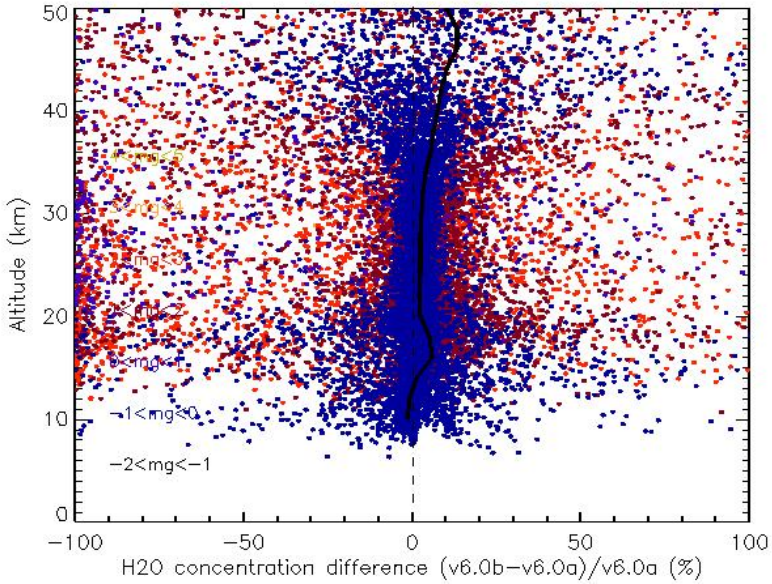

Figure 7.4-2: Values of the difference between H_2O concentration values processed with GOPR v6.0b6.0a and GOPR v6.0a6.0a for 2000 full dark occultations of cycle 22; vertical profile of the median of the difference (solid line) (updated from previous QWG report). The colour code according to the star magnitude is as follows: -2 < mg < -1; -1 < mg < 0; 0 < mg < 1 ; 1 < mg < 2; 2 < mg < 3; 3 < mg < 4; 4 < mg < 5

7.5 Inter-Comparison with external data

Results will be presented upon availability.